NAVAL POSTGRADUATE SCHOOL
Monterey, California

THESIS

CONSTRUCTION AND QUANTIFICATION OF A TOROIDAL BUBBLE APPARATUS

by

Allen L. Hobbs

September 2000

Thesis Advisor: Bruce C. Denardo
Second Reader: Andrés Larraza

Approved for public release; distribution is unlimited

REPORT DOCUMENTATION PAGE			Form Approved OMB No. 0704-0188

Public reporting burden for this collection of information is estimated to average 1 hour per response, including the time for reviewing instruction, searching existing data sources, gathering and maintaining the data needed, and completing and reviewing the collection of information. Send comments regarding this burden estimate or any other aspect of this collection of information, including suggestions for reducing this burden, to Washington Headquarters Services, Directorate for Information Operations and Reports, 1215 Jefferson Davis Highway, Suite 1204, Arlington VA 22202-4302, and to the Office of Management and Budget, Paperwork Reduction Project (0704-0188), Washington DC 20503.

1. AGENCY USE ONLY *(Leave blank)*	2. REPORT DATE	3. REPORT TYPE AND DATES COVERED
	September 2000	Master's Thesis

4. TITLE AND SUBTITLE: Construction and Quantification of a Toroidal Bubble Apparatus	5. FUNDING NUMBERS
6. AUTHOR: Hobbs, Allen L.	
7. PERFORMING ORGANIZATION NAME(S) AND ADDRESS(ES) Naval Postgraduate School Monterey, CA 93943-5000	8. PERFORMING ORGANIZATION REPORT NUMBER
9. SPONSORING / MONITORING AGENCY NAME(S) AND ADDRESS(ES) N/A	10. SPONSORING / MONITORING AGENCY REPORT NUMBER

11. SUPPLEMENTARY NOTES The views expressed in this thesis are those of the author and do not reflect the official policy or position of the Department of Defense or the U.S. Government.

12a. DISTRIBUTION / AVAILABILITY STATEMENT	12b. DISTRIBUTION CODE
Approved for pulic release; distribution is unlimited	A

13. ABSTRACT *(maximum 200 words)*

A toroidal bubble is a vortex ring with a gas core in a liquid. Current interest in toroidal bubbles is partially due to the discovery that small toroidal bubbles can occur in the cavitation collapse of a spherical bubble near the surface of a solid. This can occur near a propeller blade, causing both damage and acoustic emission. Another motivation is that dolphins generate a rich variety of large vortex bubbles. The objectives of this thesis are the construction of an apparatus that generates large toroidal bubbles in a tank of water, and the establishment of the parameter space in which toroidal bubbles occur. The apparatus employs a variable electrical input, interchangeable solenoid valve, interchangeable needle valve, and pressurized nitrogen gas. The tank is an acrylic cylinder with diameter one foot and height four feet. It is observed that whether or not a toroidal bubble forms is highly stochastic. This is studied by varying several parameters of the apparatus. Preliminary results of possible acoustic emission are presented. Future work with the apparatus is discussed, including digital photography of toroidal bubble formation and the effect on ensonification on the motion.

14. SUBJECT TERMS: Toroidal Bubble, Vortex Ring, Acoustic Emission	15. NUMBER OF PAGES: 122
	16. PRICE CODE

17. SECURITY CLASSIFICATION OF REPORT	18. SECURITY CLASSIFICATION OF THIS PAGE	19. SECURITY CLASSIFICATION OF ABSTRACT	20. LIMITATION OF ABSTRACT
Unclassified	Unclassified	Unclassified	UL

NSN 7540-01-280-5500 Standard Form 298 (Rev. 2-89)
Prescribed by ANSI Std. 239-18

THIS PAGE INTENTIONALLY LEFT BLANK

Approved for public release; distribution is unlimited

CONSTRUCTION AND QUANTIFICATION OF A TOROIDAL BUBBLE APPARATUS

Allen L. Hobbs
Lieutenant, United States Navy
B.S., United States Naval Academy, 1993

Submitted in partial fulfillment of the
requirements for the degree of

MASTER OF SCIENCE IN ENGINEERING ACOUSTICS

from the

NAVAL POSTGRADUATE SCHOOL
September 2000

Author: _____
Allen L. Hobbs

Approved: _____
Bruce C. Denardo, Thesis Advisor

_____
Andrés Larraza, Second Reader

_____
Kevin B. Smith, Chairman, Engineering Acoustics
Academic Committee

THIS PAGE INTENTIONALLY LEFT BLANK

ABSTRACT

A toroidal bubble is a vortex ring with a gas core in a liquid. Current interest in toroidal bubbles is partially due to the discovery that small toroidal bubbles can occur in the cavitation collapse of a spherical bubble near the surface of a solid. This can occur near a propeller blade, causing both damage and acoustic emission. Another motivation is that dolphins generate a rich variety of large vortex bubbles. The objectives of this thesis are the construction of an apparatus that generates large toroidal bubbles in a tank of water, and the establishment of the parameter space in which toroidal bubbles occur. The apparatus employs a variable electrical input, interchangeable solenoid valve, interchangeable needle valve, and pressurized nitrogen gas. The tank is an acrylic cylinder with diameter one foot and height four feet. It is observed that whether or not a toroidal bubble forms is highly stochastic. This is studied by varying several parameters of the apparatus. Preliminary results of possible acoustic emission are presented. Future work with the apparatus is discussed, including sequential digital photography of toroidal bubble formation and the effect of ensonification on the motion.

THIS PAGE INTENTIONALLY LEFT BLANK

TABLE OF CONTENTS

LIST OF FIGURES

LIST OF TABLES

THIS PAGE INTENTIONALLY LEFT BLANK

ACKNOWLEDGEMENTS

My work at the Naval Postgraduate School is dedicated to my grandfather, Joe Rubio, and great uncle, Roy Garcia, both veterans of World War II.

Thesis planning, experimentation and writing are not trivial tasks. Many factors are involved, some tangible and some not. One intangible but essential factor is support. My family and the Naval Postgraduate School staff helped in many situations. Their encouragement, guidance and expertise enabled me to achieve a worthwhile product: the completed thesis.

My wife and children spent many evenings alone at home while I labored in Spanagel 015, my thesis workspace. For their patience and understanding, I thank Carie, Marshall and Elizabeth. My accomplishment is theirs, also.

Professor Bruce Denardo, my thesis advisor, conducted extensive research on vortex rings and toroidal bubbles. He expertly directed my efforts and shaped the thesis into a readable, technically accurate document. He taught me to be patient in research. Modelmaker George Jaksha conceived of and built some remarkable hardware components for the apparatus. I admire his ability to design and create a working mechanical device from only a concept.

My Curricular Officer and friend, Commander Jim Hill, supported me during the long walk to thesis completion and graduation. I will always remember his guidance and fairness.

Finally and most importantly, I thank God for enabling me to complete this thesis and graduate from the Naval Postgraduate School.

THIS PAGE INTENTIONALLY LEFT BLANK

I. INTRODUCTION

Vortex motion of fluids is readily observed and demonstrated. This has fascinated people for many centuries, as evidenced by stories of giant whirlpools that have swallowed ships. Descartes originated a theory in which vortices were responsible for planetary motion. Extensive analytical development of vortices occurred in the second half of the 1800s due to prominent physicists Helmholtz, Kelvin, J. J. Thompson and others (Lamb, 1997). Remarkably, Kelvin proposed a theory of atoms based on vortex rings in the ether (Acheson, 1990).

A recent example of vortex motion is the observation of "dust devils" (small tornadoes) on the surface of Mars (Metzer, 2000). These pairs of dust devils typically have oppositely directed circulations, causing them to translate rather than rotate. In superfluid helium (^{4}He), quantized vortex lines and rings can occur (Putterman, 1974; Reif, 1964; Faber, 1995) and elementary excitations referred to as *rotons* may be microscopic vortex rings (Faber, 1995). Quantized vortices in a stirred Bose-Einstein condensate have recently been observed (Fitzgerald, 2000).

A *toroidal vortex ring* can be defined as a vortex ring containing a core of different fluid than the surrounding fluid. A standard vortex ring is the limiting case in which the two fluids are the same. This can be beautifully demonstrated by a smoke ring, which can easily be produced with a large cardboard box. A four-inch (approximate) diameter hole is cut at the center of the front face. The cardboard is removed from the back face, and the opening is covered with a thin

plastic sheet that is taped to the box. The sheet is tapped to produce vortex rings. Though the vortex ring is not visible, a person can feel the vortex ring with an opened hand. Smoke from a fog machine can be fed into the front hole, and the back again tapped by hand. This produces a dramatic, visual, well defined vortex ring (the smoke is drawn to the region near the core by the lower pressure; in the core the flow is rotational and Bernoulli does not apply). The flow of a vortex ring can easily extinguish the flame on a distant (10-15 *ft* away) candle. It should be noted that the vortex ring is still composed of air; the smoke only serves to outline its boundary. Visual, standard vortex rings can also be demonstrated by allowing drops of colored water to strike a still water surface (Batchelor, 1967). Experiments have been conducted on such drop-generated vortex rings (Shankar, 1995). Toroidal vortex rings can be demonstrated by employing a dissimilar liquid (for example, Pepto Bismal™ or colored salt water) as the drops (Reif, 1964). The mushroom effect of explosions motivated an early investigation of toroidal vortex rings (Turner, 1957). The heat due to the explosion causes the air convected by the vortex ring to have less density than the surrounding air. A motivation for this investigation was the possibility of employing vortex rings to seed clouds to produce rain.

This thesis is concerned with a *toroidal bubble*, which is a special case of a toroidal vortex ring with a gaseous core in a liquid. Current interest in toroidal bubbles is partially due to the discovery that small toroidal bubbles can form from the cavitation collapse of a spherical bubble near the surface of a solid (Blake, 1999; Sussman, 1997). This can occur near a propeller blade, causing

both damage and acoustic emission. Another motivation is the discovery that dolphins generate a rich variety of large vortex bubbles (Marten, et al., 1996).

There is a significant amount of analytical (Turner, 1957; Pedley, 1968; Lundgren, 1991) and numerical (Lundgren, 1991; Chen, 1999; Sussman, 1997) work related to large toroidal bubbles. In contrast, there are apparently only two experimental investigations (Walters, 1963; Turner, 1957), which make only brief remarks about a toroidal bubble-producing apparatus. The main objectives of this thesis are the construction of an apparatus that generates large toroidal bubbles in a tank of water, and the establishment of the parameter space for which toroidal bubbles occur. An interesting result is that whether or not a toroidal bubble forms is highly stochastic, which is not surprising due to the very turbulent nature of the formative burst of gas. To study the stochastic nature of the toroidal bubble, some drive plane parameters of the apparatus are manipulated to form such bubbles. Another motivation is the possible acoustic emission due to volume oscillations of a toroidal bubble. These oscillations are expected to occur as a result of the formation. Preliminary measurements of this are reported. Future work with the apparatus is discussed, including digital photography of toroidal bubble formation and propagation, as well as the effect of external sound on toroidal bubble motion. Future work involving the construction of a hands-on apparatus for the public is also discussed. The Exploratorium, a science museum in San Francisco, California in the 1980s, had a toroidal bubble display, but the apparatus was not hands-on, and is only briefly described in the literature (Semper, 1992).

THIS PAGE INTENTIONALLY LEFT BLANK

II. THEORY

A vortex can exist in any fluid, whether liquid or gas. All vortices are composed of a fluid that rotates around a core. The vorticity vanishes outside the core and is nonzero inside. The core may or may not be composed of the same fluid as that outside.

A. FUNDAMENTALS

Figure II.1 shows the typically measured parameters of a line vortex. The velocity of a discrete point outside the core is inversely proportional to distance measured radially from the axial center.

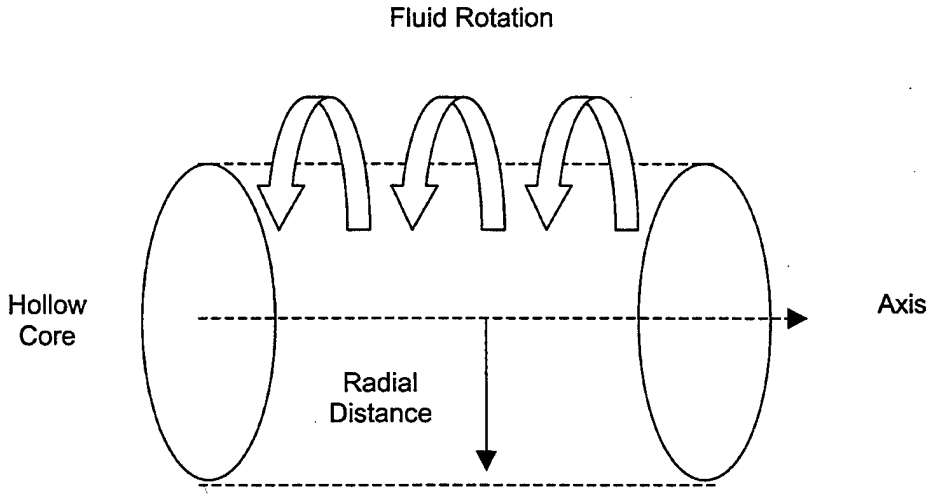

Figure II.1. Basic geometry of a line vortex.

The relationship between velocity and radial distance is expressed as $v = K/r$, where v is the velocity of fluid particle, K is the vortex strength, and r is the radial distance from the axis to the fluid particle. The strength of the vortex is expressed as the constant of proportionality. It does not change with time in an inviscid fluid. Its magnitude depends on how much energy was initially imparted to the rotational motion of the vortex.

The core of a vortex can be straight or curved. In particular, it can be bent around and joined end to end to form a ring. This thesis is concerned with toroidal bubbles, which are vortex rings with a gaseous core in a liquid. The liquid particles revolve about this core.

Fluid particle velocity directly influences the velocity at which a vortex ring moves through a fluid. By Kelvin's circulation theorem, any section of a vortex core must move with the local fluid velocity. Hence, vortex ring motion through a fluid medium is always perpendicular to the plane in which the longitudinal axis lies. However, external forces can alter the shape and the motion, as shown in Figures II.2 and II.3. The reason for the expansion in Figure II.2 is that the force does work on the ring and thus increases its energy, and that the ring radius increases with energy. For a ring of constant vortex strength, the speed of the ring decreases with energy. Hence, the bigger the ring, the more slowly it moves through the fluid (Reif, 1964).

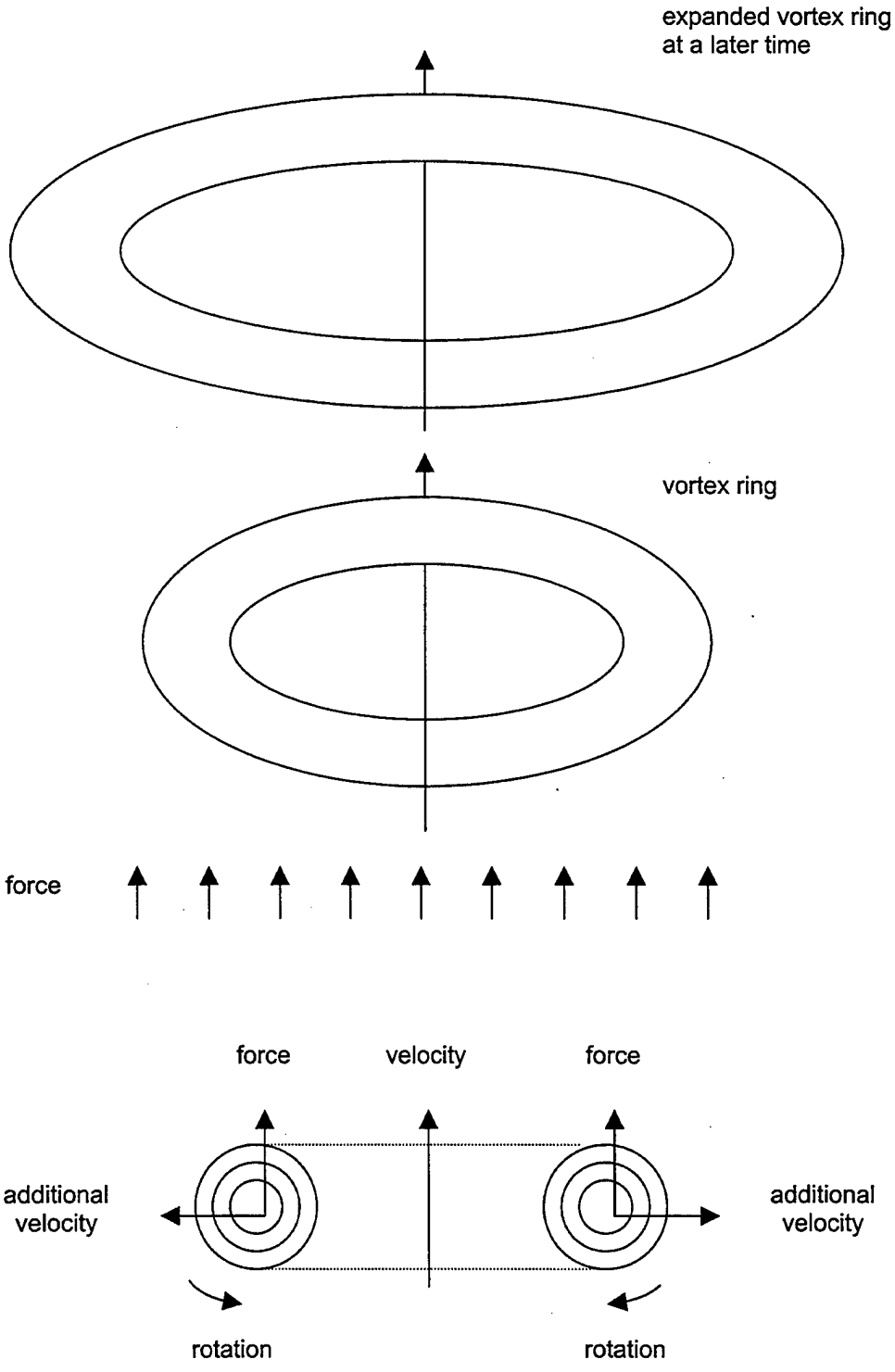

Figure II.2. Perpendicular force acting on a ring vortex. Expansion of a vortex ring results from an external force (such as buoyancy) acting at right angles to the plane of the ring. Effects of such a perpendicular force are shown in the cross-sectional view. (Reif, 1964)

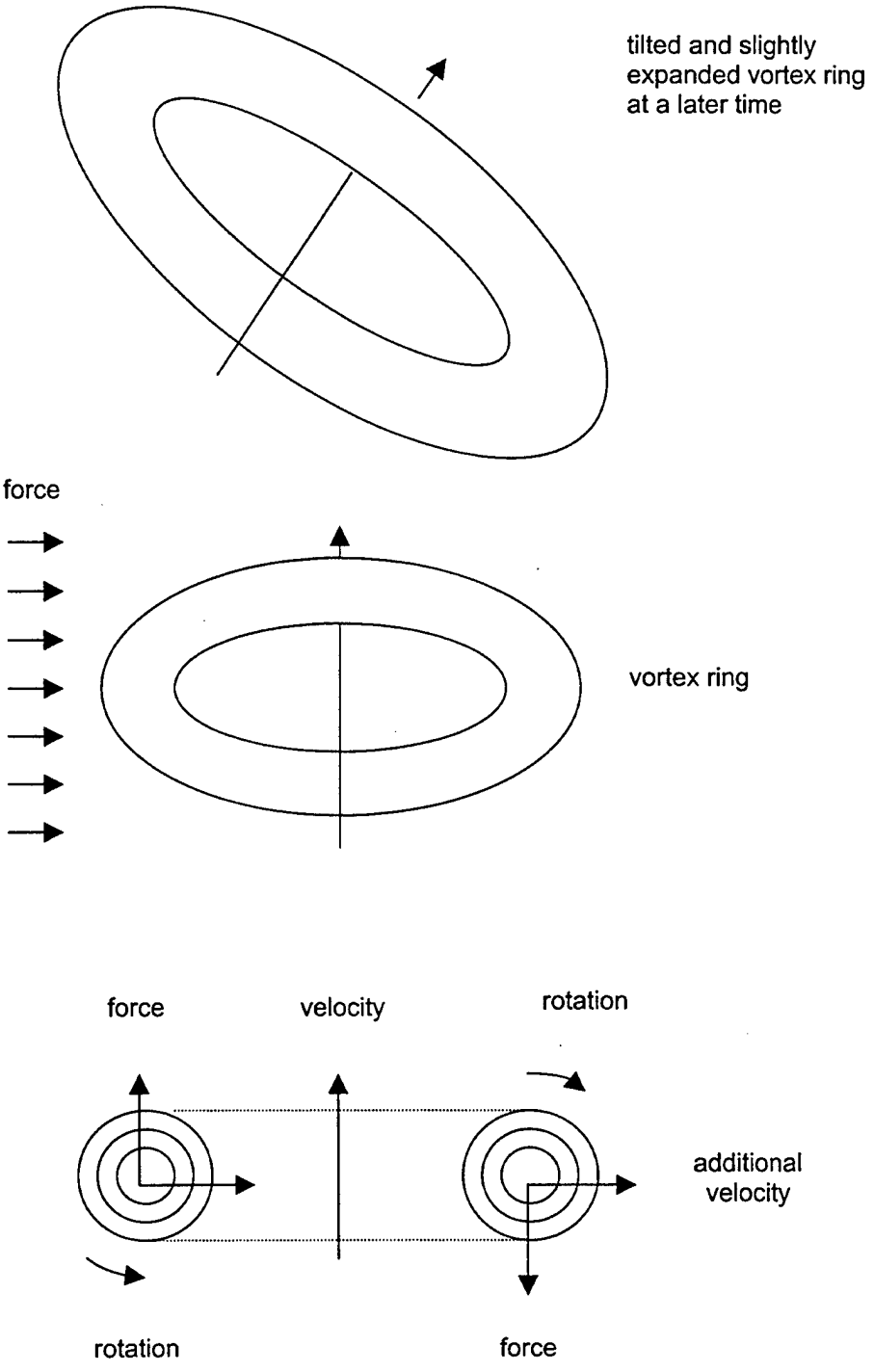

Figure II.3. Parallel force acting on a ring vortex. Tilting of a vortex ring occurs when an external force acts parallel to the plane of the ring. Effects of such a parallel force are shown in the cross-sectional view. (Reif, 1964)

B. CONSERVATION OF VOLUME

Though the toroidal bubble changes shape as it moves through the fluid medium, it is important to note that its volume remains approximately the same. The hydrostatic pressure changes little over distances of roughly 1 *m*, and the Bernoulli effect, due to increasing fluid velocity at the boundary of the shrinking core, is negligible. Furthermore, no gas is lost to the surrounding fluid.

C. MOVEMENT WITHIN A FLUID

This experiment uses a 4 *ft* long tube filled with tap water. Before discussion can be made about the movement of a toroidal bubble through the water column, general vortex movements through liquid must be described.

If a vortex ring core were composed of the same fluid contained in the water column, the vortex ring would be subject to no net external forces. Theoretically, it would move through the water column with no change in size or velocity.

A vortex ring composed of a heavier liquid than pure water will act quite differently. Consider the example of a salt water vortex ring moving through pure water. Since salt water is heavier than pure water, a net gravitational force greater than the buoyant force pushes the ring downward. As the ring moves downward, it increases in size and decreases in speed. This movement has been observed. (Reif, 1964)

The vortex ring core in this experiment is composed of nitrogen, and is much less dense than a liquid vortex ring. The formation and movement of this toroidal bubble can readily be seen in the water column. It moves upward through the 4 *ft* tall water column because of its buoyancy and its flow field; its diameter increases with time.

D. EXAMPLES IN NATURE

Easily observed toroidal bubbles in nature are created by dolphins. Sea Life Park Hawaii has made extensive observations of its dolphins creating single and double toroidal bubbles. (Marten, et al., 1996)

One male dolphin routinely produces a ring of air just to watch it rise to the surface. Each toroidal bubble originates at the dolphin's blowhole and remains stable as it rises to the surface. The same dolphin occasionally emits two rings in succession. The rings fuse into a large toroidal bubble. As theory predicts, this single toroidal bubble becomes thinner and expands in diameter as it rises to the surface. The vortex flow combines with the buoyant force to drive the toroidal bubble to the surface. The same vortex flow also stabilizes the toroidal bubble, preventing it from disintegrating into spherical bubbles.

Another dolphin at Sea Life Park Hawaii, a female, typically creates a vortex in the water by sharply moving its tail fin through the water, causing a vortex action. The dolphin then exhales into the vortex. The vortex draws the air into its center, forming a toroidal bubble that moves horizontally and slightly downward through the water.

Toroidal bubbles created by dolphins are only a fraction of the vortex actions that occur in the physical world. Small toroidal bubbles can occur due to the cavitation collapse of a spherical bubble near a solid surface. Quantized vortex rings can occur in superfluid helium. These vortex actions help describe and predict the toroidal bubbles created in this experiment.

E. FUNDAMENTAL EQUATIONS

Any vortex ring contains a definite kinetic energy per unit length because of the circulation of fluid around the vortex core. The velocity of a vortex ring moving through a bounding fluid is inversely proportional to its diameter. Because of this relationship, the velocity decreases with kinetic energy. The kinetic energy and velocity of a vortex ring can be calculated using the following equations (Putterman, 1974):

$$E_k = (2\pi^2)(\rho\gamma^2)R\left[\ln\left(\frac{8R}{a}\right) - 2\right]$$

$$v = \left(\frac{\gamma}{2R}\right)\left[\ln\left(\frac{8R}{a}\right) - \frac{1}{2}\right]$$

E_k - kinetic energy of vortex ring (J)

v - velocity of the vortex ring through an incompressible fluid ($\frac{m}{s}$)

ρ - density of the incompressible fluid ($\frac{kg}{m^3}$)

$2\pi\gamma$ - circulation of any contour that encircles the vortex core

R - vortex ring radius (m)

a - vortex core radius (m)

The circulation $2\pi\gamma$ around the vortex core applies to all fluid particles in rotation. In this experiment, these particles are water molecules that rotate around the bounded nitrogen gas in the vortex core. Of importance is the relationship $v \sim 1/E_k$. Consider a toroidal bubble with constant circulation around the vortex core. If such a toroidal bubble receives energy (is acted upon by an external force), it does not accelerate as a unit, but increases in size. This increase in diameter actually causes a deceleration of the toroidal bubble. As previously stated, volume remains conserved.

To use the previous two equations, the fluid surrounding the vortex ring must be incompressible and infinite. The water column is considered to be infinite and incompressible.

III. APPARATUS

Figure III.1 depicts the apparatus. Its design and fabrication posed a challenge; many components needed to be integrated into a dedicated system capable of producing a single, gaseous toroidal bubble in a liquid column. Though the study of toroidal bubble production is known to be highly empirical, construction of the apparatus was based on two supporting factors: the initial work supervised by Kolaini and Denardo (University of Mississippi, 1994-1996), and the machining expertise of Jaksha (Modelmaker, Naval Postgraduate School).

The apparatus uses nitrogen and water as the working fluids. The system consists of three distinct subsystems: electrical, gas and liquid. The electrical subsystem includes a function generator coupled to a power supply amplifier, and an electronics box. The gas subsystem includes a nitrogen supply cylinder, various pressure regulators and a pressure reservoir. The liquid subsystem includes a rigid frame and transparent, thin-walled tank. The single component that integrates the electrical, gas and liquid subsystems is the electro-mechanical solenoid valve. This central node uses an electrical control signal to regulate the flow of compressed nitrogen into a nozzle assembly within the tank. This nozzle assembly is the mechanical interface between gas and liquid.

The following sections describe each component of the apparatus, as shown in Figures III.1 – III.5. Detailed analysis of some components is essential as toroidal bubble production is influenced by several adjustable factors.

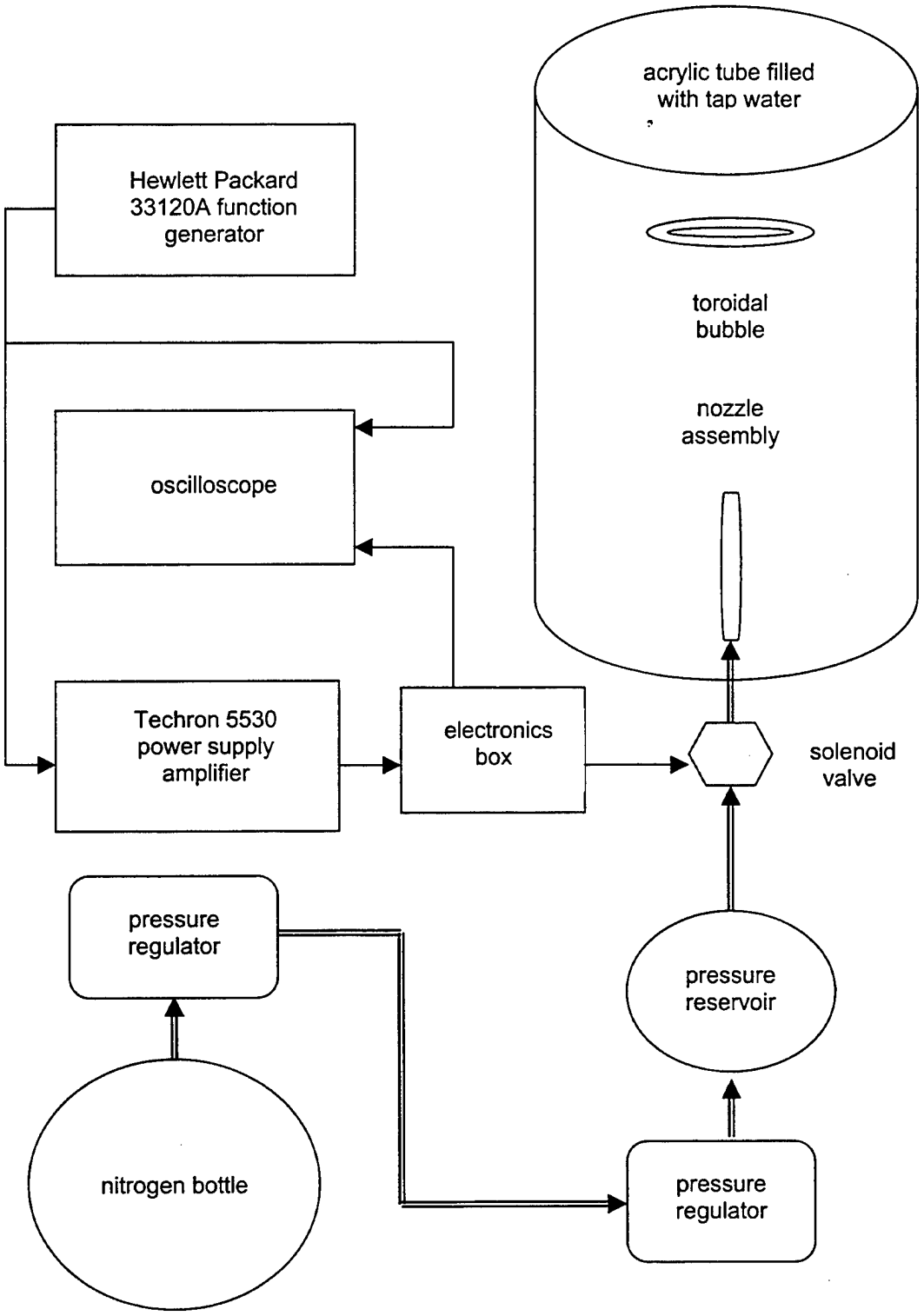

Figure III.1. Block diagram of entire toroidal bubble apparatus.

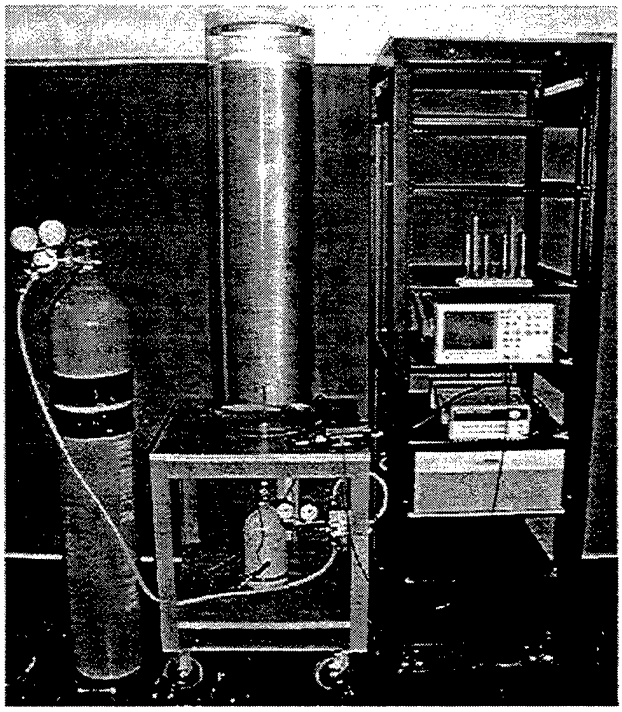

Figure III.2. Entire toroidal bubble apparatus with nitrogen bottle, equipment rack and nozzle assemblies.

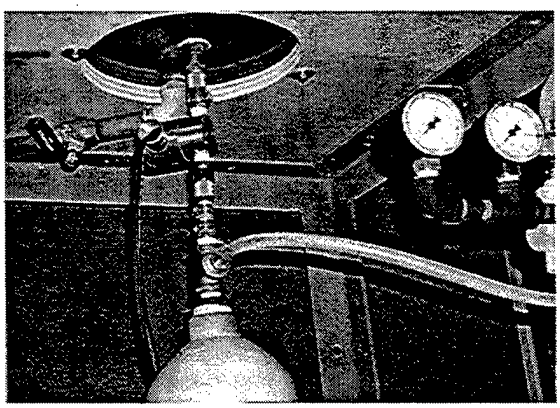

Figure III.3. Components directly beneath *PVC* disk, including solenoid valve, drain valve, pressure reservoir, and pressure regulator with gauges. Luer fittings connect hoses to the penetrating bolt, solenoid valve and pressure reservoir.

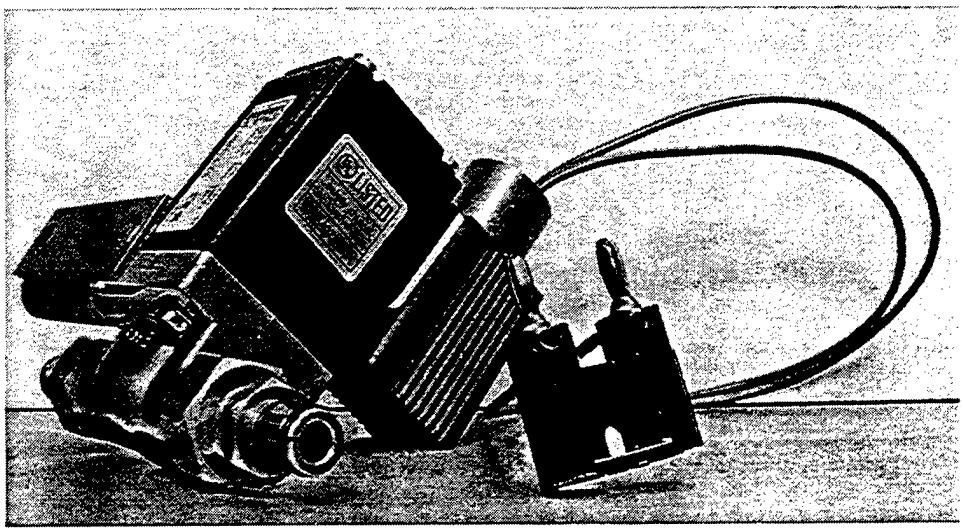

Figure III.4. Burkert solenoid valve.

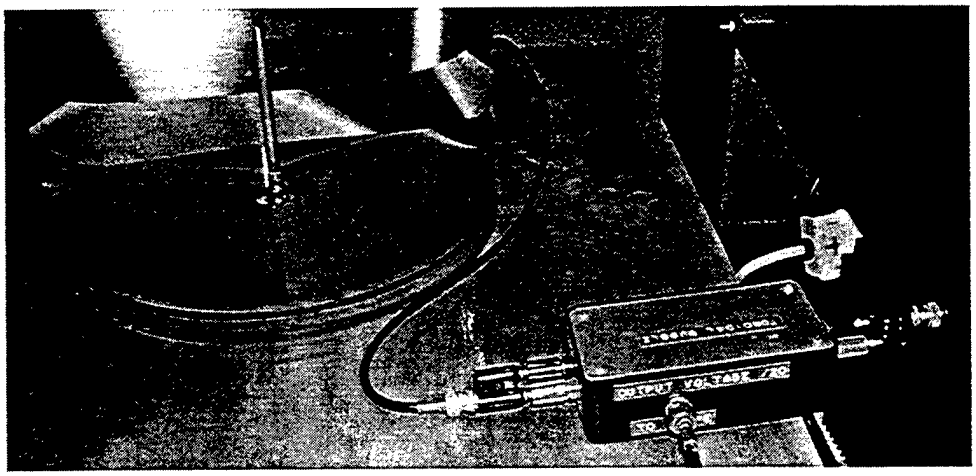

Figure III.5. In-water nozzle assembly and dual purpose electronics box.

In the apparatus, the following critical parameters are adjustable:

- nitrogen pressure
- solenoid valve open time (length of nitrogen burst)
- time between nitrogen bursts
- nozzle diameter
- nozzle length

A. FUNCTION GENERATOR

The action of a solenoid valve controls the flow of pressurized nitrogen into a vertically oriented, right-cylindrical water column bounded by an acrylic tube. Under certain conditions, this burst of rapidly expanding nitrogen produces a toroidal bubble. A function generator and power amplifier control the solenoid valve. The solenoid valve is electromechanical in nature, converting electrical energy to mechanical energy in the toroidal bubble production process.

The solenoid valve must have the proper electrical signal to produce a toroidal bubble. This electrical signal must be of sufficient voltage and waveform to drive the valve to specifications. The Hewlett Packard 33120A function generator and the Techron 5530 power supply amplifier can accomplish this. The experiment calls for the production of a tightly formed toroidal bubble. To produce this output, the function generator must provide a known, programmed input signal to the power supply amplifier. The power supply amplifier must then step up the voltage and supply the current to overcome the

spring force that holds the valve in its closed, default position. After opening the valve, the electrical signal must then hold the solenoid valve open for a certain time to allow a pre-specified flow of nitrogen into the needle valve. A modified rectangular wave signal accomplishes this.

The function generator is a digital device capable of producing a variety of output signals. With some manipulation, this function generator produces the modified rectangular wave required for proper solenoid valve operation.

In the burst mode, the function generator produces the generic sinusoidal output shown in Figure III.6. Based on this sinusoidal form, the rectangular wave output is expected to be as shown in Figure III.7. However, the function generator produces a very different rectangular wave than that in Figure III.7. The Hewlett Packard 33120A, as most function generators commercially available, produces a pseudo-rectangular wave output. The actual output is shown in Figure III.8.

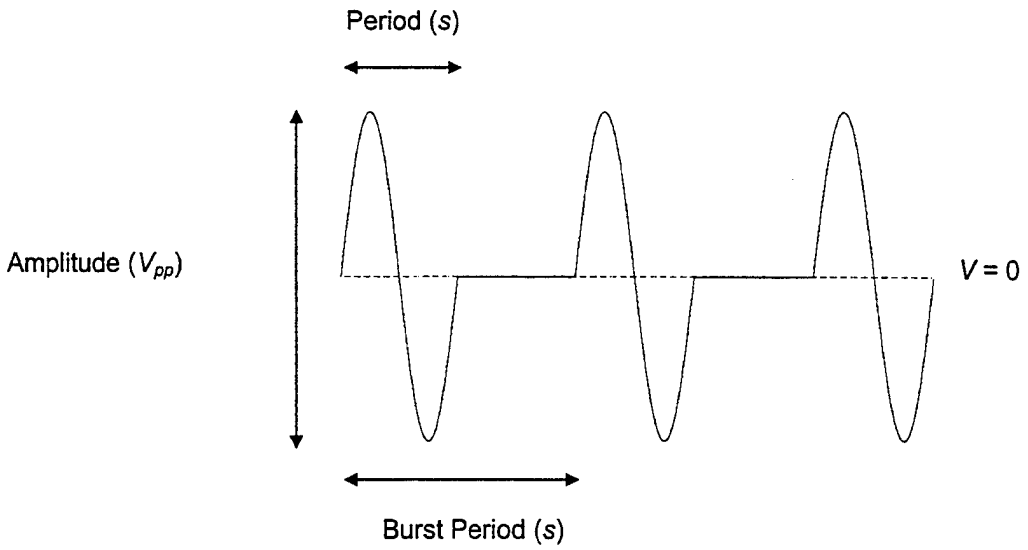

Figure III.6. Full period sine wave, occurring at periodic intervals.

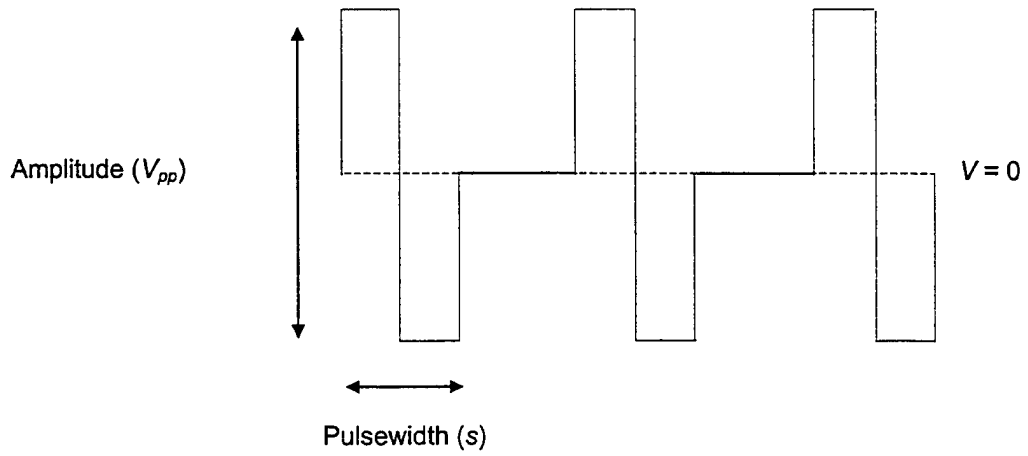

Figure III.7. Anticipated rectangular wave, occurring at periodic intervals.

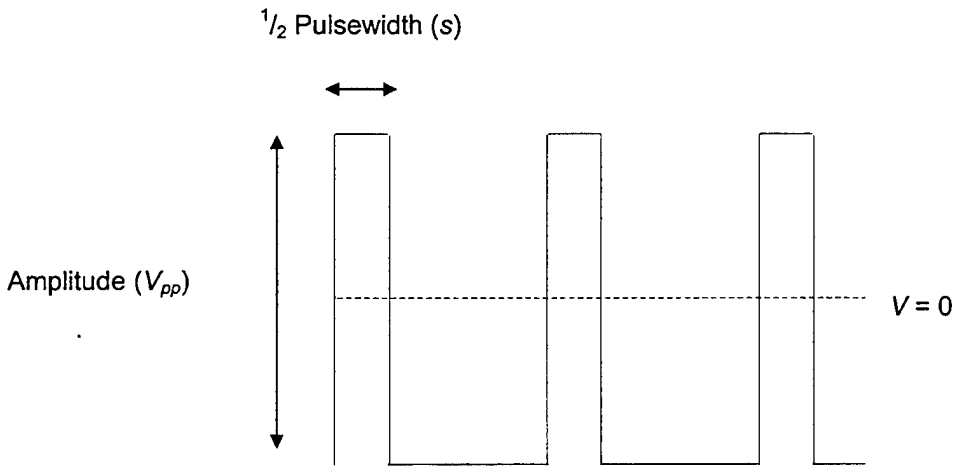

Figure III.8. Actual rectangular wave, occurring at periodic intervals

The following actions were taken to produce the desired rectangular wave output and to provide an accurate history of the output electrical signal:

- The function generator output must be consistently recorded as voltage peak-to-peak (V_{pp}) or voltage root mean square (V_{rms}).
- Since the pseudo-square wave zero voltage levels fall below the actual zero voltage axis by $^1/_2$ its amplitude, this wave must be offset positively by $^1/_2$ its amplitude.
- Because the pseudo-square wave on-time is $^1/_2$ that expected (when compared to a simple sinusoid), pulse duration must be doubled (for example, a 10 *ms* on-time requires a 20 *ms* setting).

B. POWER SUPPLY AMPLIFIER

The Techron 5530 power supply amplifier is a dual mode amplifier that is capable of independently amplifying electrical signals through two channels or amplifying through a single, bridged channel (monaural output). The power supply amplifier is normally operated in dual channel mode, in which each amplifier channel is separate. If more power is needed for a single channel, the Techron 5530 power supply amplifier can be bridged into a monaural mode.

The power supply amplifier can be thought of as a lumped electrical element, which presents a large electrical resistance to the input signal. This large resistance, on the order of 1 $M\Omega$, allows the function generator to output its electrical signal at a known, stable voltage. This relationship is Ohm's Law in its simplest form: $V = I \times R$. The function generator need not supply appreciable current to the power supply amplifier.

C. SOLENOID VALVE

A solenoid valve controls the flow of pressurized nitrogen into the nozzle assembly prior to entering the water column. This solenoid valve is electrically operated. The function generator provides a voltage signal to the power supply amplifier, which amplifies the signal to drive the solenoid valve. The solenoid valve is critical to the toroidal bubble formation process. This key component controls the volume of nitrogen that flows into the water column via the nozzle assembly.

Skinner Valve Division, Honeywell, manufactures a prototypical solenoid valve that is electrically opened and mechanically closed. This type of solenoid valve is shown in Figure III.9, and includes the following components:

- pressure chamber
- metal plunger
- electromagnetic coil with electrical leads
- mechanical spring and internal O-ring
- stem with threaded base
- outer case with opening for electrical leads

These components fit together to form a solenoid valve that is utilized, in our case, to precisely control the flow of pressurized nitrogen gas. Specifically, the solenoid valve allows a specific volume of pressurized nitrogen to flow from the pressure reservoir to the water chamber.

The pressure reservoir is designed to operate at about 1-17 *psi*. Note that some pressure losses occur in the system due to drag along the inner tube walls and hose connectors. More complicated pressure and velocity changes occur within the solenoid valve and nozzle assembly. The opening and closing actions of a metal plunger necessarily cause differential nitrogen flow rates during each open-close cycle.

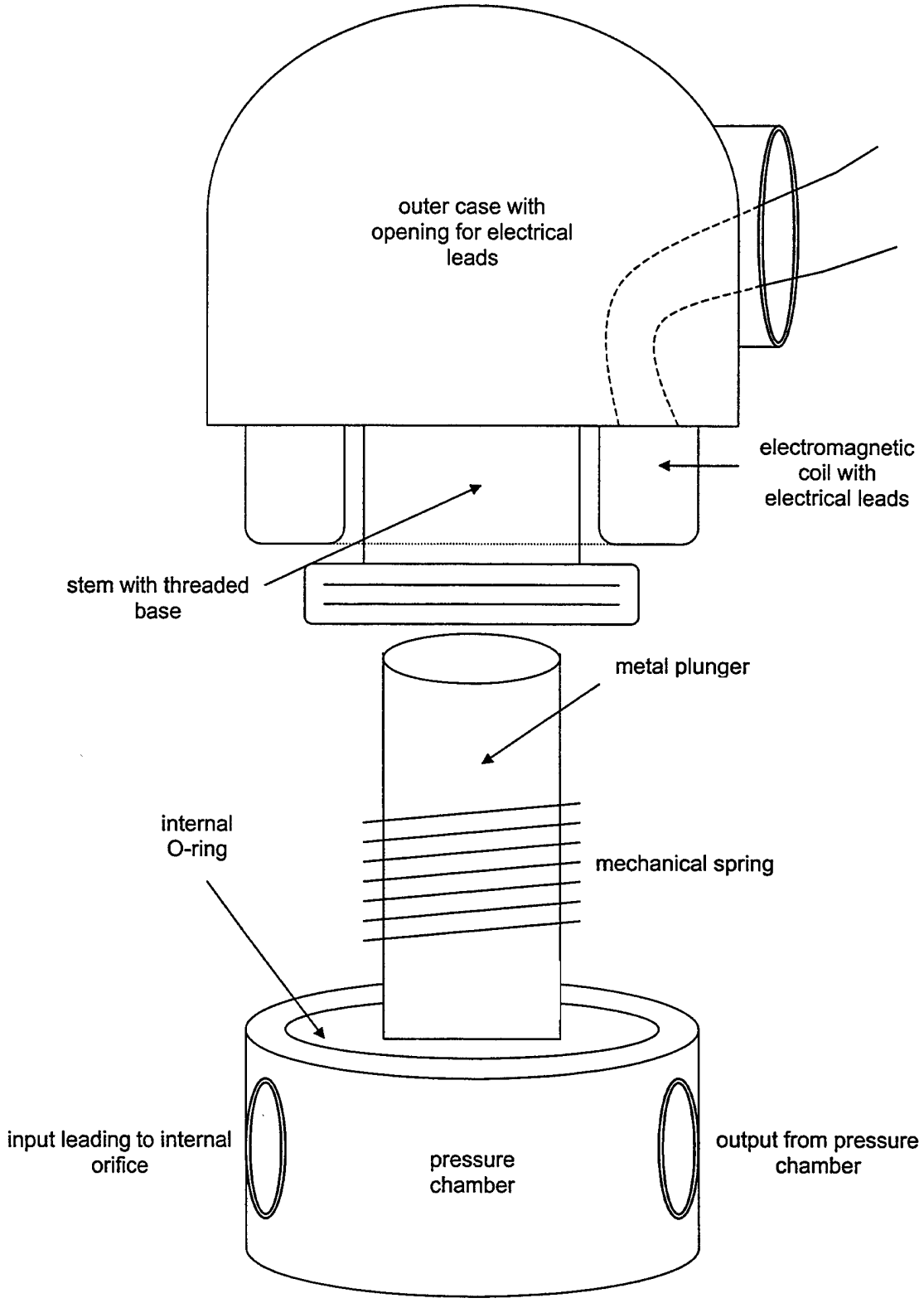

Figure III.9. Exploded view of a typical solenoid valve.

The metal plunger physically controls the flow of pressurized nitrogen through the pressure chamber. It fits inside the stem and moves in one dimension only. It is the mechanical method by which nitrogen flow is started and stopped. The metal plunger operates within a magnetic field created when current passes through the magnetic coil. This magnetic field causes the opening action of the solenoid valve by causing the metal plunger to lift off the centered opening in the pressure chamber bottom.

The plunger remains in the raised position as long as the minimum threshold current is supplied to the electromagnetic coil. A mechanical spring fits around the metal plunger and acts against the magnetic field as the metal plunger opens. The spring must be relatively weak to not overpower the force of the magnetic field. For this reason, the spring is limited in its ability to impulsively throw the valve closed when required.

The pressure chamber is continuous-cast and contains two external openings. These external openings are threaded to standard $^{1}/_{4}$" *NPT* pipe size. One opening allows the input of pressurized fluid; the other opening controls the output of pressurized fluid. As noted previously, this fluid is gaseous nitrogen.

The smooth walled conduit between the external input opening and the pressure chamber is known as the orifice. The orifice is also measured in standard *NPT* pipe size. The input orifice is angled downward from the external input to the pressure chamber. This orifice is designed as a neutral input; it does not directly oppose or aid the plunger.

The output external opening is also connected to the pressure chamber by a smooth walled orifice. Like the input orifice, it is standard $^1/_4$" *NPT* size. The output orifice connects to the pressure chamber base by a centered opening in its bottom. This centered opening makes contact with the metal plunger when the valve is closed.

If the other external opening were used as the output side, the centered opening would directly oppose the plunger when closing and aid the plunger when opening. This arrangement would be unacceptable since stoppage of nitrogen flow occurs more slowly than flow start for our application.

D. DUAL PURPOSE ELECTRONICS BOX

The voltage signal from the power supply amplifier is relayed to the solenoid valve through an electronics box. Shown in Figure III.5 and III.10, the electronics box has two parts. The first part is a voltage divider, which reduces the voltage from the power amplifier to the oscilloscope. This is necessary because the voltage required to activate the solenoid valve is typically 50 V_{pp}, which exceeds the display limit of the oscilloscope. The electrical resistance $R_1 + R_2$ is chosen to be large so that very little current passes through it. The voltage to the oscilloscope is reduced by the factor $1/(1+R_1/R_2)$. The ratio of the resistances is chosen to be $R_1/R_2 = 9.0$, so that the voltage to the oscilloscope is reduced by a factor of 10.0. Our resistances are $R_1 = 8.9\ k\Omega$ and $R_2 = 0.99\ k\Omega$.

The second part of the electronics box is a diode which acts to protect the amplifier from possible damage due to the abrupt voltage drop in solenoid valve

coil. Induction in the coil causes the current to continue after the amplified voltage drops to zero. The inductance and *DC* resistance of the solenoid valve were measured to be 0.40 *H* and 135 Ω, respectively. The presence of the diode allows a closed path for this current, which dissipates due to the resistance of the coil.

The electronics box in Figure III.11 functions for the case of a unipolar amplifier output (one terminal grounded). This case occurs for a single channel of a dual channel amplifier. If such an amplifier is in the bridged (monaural) mode, a bipolar output occurs. This bipolar output should not be directly connected to an oscilloscope because the outer conductors of oscilloscope terminals are nearly always grounded. In this case, a large current would then flow through the wire to the ground on the oscilloscope. As shown in Figure III.11, a solution to this problem is to disconnect the wire and the end of R_2 from the conductor that was previously grounded by the amplifier, then connect the wire and R_2. The voltage to the oscilloscope is then reduced by a factor of 20.0 rather than 10.0, assuming the oscilloscope and amplifier have a common ground.

Our experiment did not require the monaural mode. A future experiment will modify the solenoid valve by using a stiffer spring to possibly improve closure time. When opening, the solenoid valve will then require a higher voltage input to overcome the additional spring force. The monaural mode will be required.

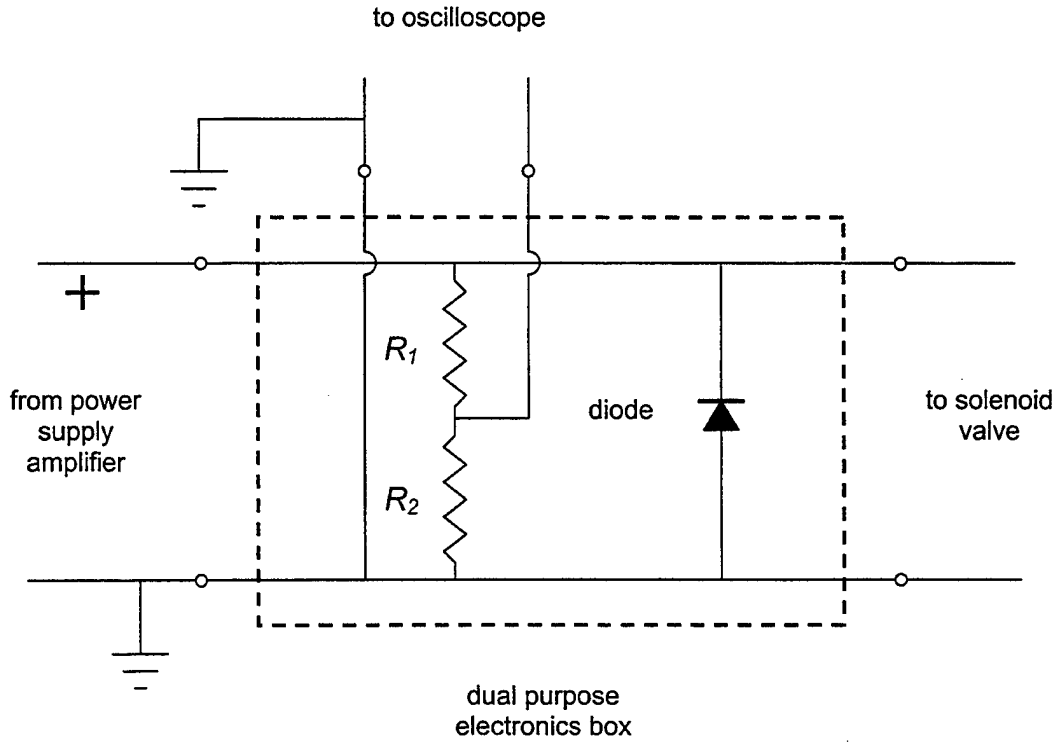

Figure III.10. Circuitry resident in dual purpose electronics box. The power supply amplifier provides an amplified, periodic rectangular pulse.

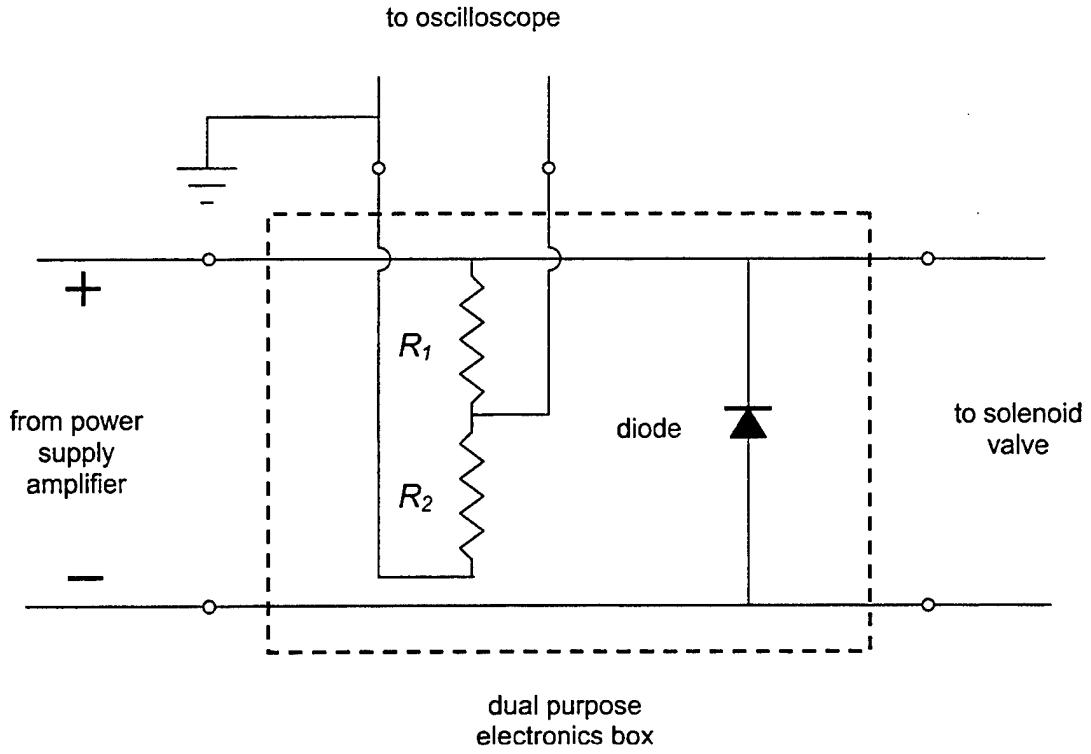

Figure III.11. Dual purpose electronics box for the case of a dual channel amplifier in the bridged (monaural) mode, so that the output is bipolar.

Note that the modified electronics box shown in Figure III.11 can also function for a unipolar amplifier output only when the oscilloscope and amplifier have a common ground.

E. SOLENOID VALVES TESTED

Two solenoid valves were initially tested for the apparatus:

- Burkett, shown in Figure III.4, distributed by Cole-Parmer (normally closed, electrically opened, mechanically closed, operated by V_{DC})

  - maximum voltage input: 24 V_{DC}
  - maximum power input: 12 *W*
  - maximum pressure input: 28 *psi*
  - orifice diameter: $^1/_4$"
  - valve number: US02633
  - valve code: 0256
  - distributor information:

  Cole-Parmer Instrument Company
  625 East Bunker Court
  Vernon Hills, Illinois 60061-1844
  (800) 323-4340

- Skinner Valve Division, distributed by Controlco (normally closed, electrically opened, mechanically closed, operated by V_{AC})

  - maximum voltage input: 120 V_{AC}
  - maximum power input: 11 *W*
  - maximum pressure input: 100 *psi*
  - orifice diameter: $^1/_8$"
  - valve number: V52LB2100
  - valve code: MC9
  - distributor information:

  Controlco Automation
  35 Dorman Avenue, Number 2
  San Francisco, California 94124
  (415) 647-9445

Details of the tests are given in Section IV.B, and Appendices A and B. The Skinner valve performed better, and was thus employed in the final version of the apparatus.

F. NOZZLE ASSEMBLY

The final, key component of the toroidal bubble apparatus is the nozzle assembly. This assembly serves the vital function of releasing pressurized nitrogen directly into the water column.

The nozzle assembly is shown in Figures III.12 – III.14. The base of the nozzle assembly is a *½" x 13-thread per inch (coarse)* brass nut. This brass nut screws onto a brass bolt that extends into the water column through the tank foundation. The brass nut is grooved in its bottom. A rubber O-ring fits into the groove to preserve watertight integrity between the nut and tank foundation. Soft silver solder holds a *⅜ — ¼"* copper sweat reducer to the brass nut. Soft silver solder also holds a *316* stainless steel tube to the copper sweat reducer. This stainless steel tube is the nozzle proper. To eliminate the effects of the relatively thick tube wall on the expanding nitrogen as it leaves the nozzle, the tube wall is tapered along its final ½" of length. A reamer was used to ensure a true inner diameter along the inner wall of the ½" taper. As a final check, a pin gauge verified this inner diameter following the manufacturing process.

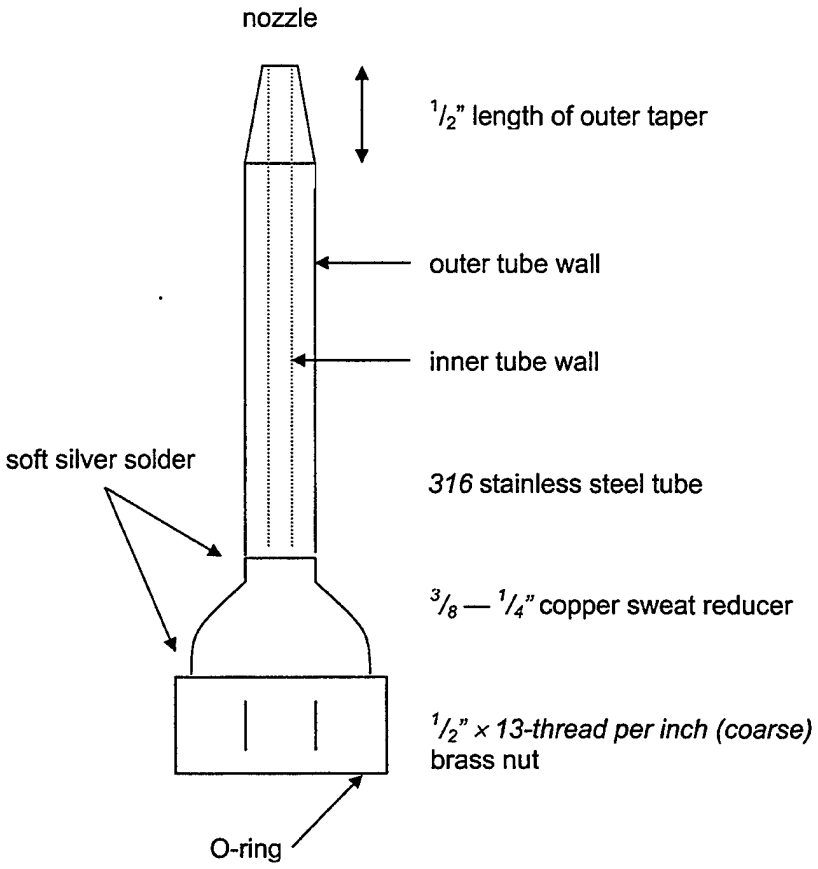

Figure III.12. In-water nozzle assembly.

Before experimentation began, a variety of configurations and dimensions were considered for the nozzle assemblies. Only parameters with a likely probability of success (tapered tip, relatively small diameter, smooth walled) were considered. Table III.1 lists the ten nozzle assemblies ultimately manufactured. All were tested to some extent, but only two were selected for follow-on experimentation.

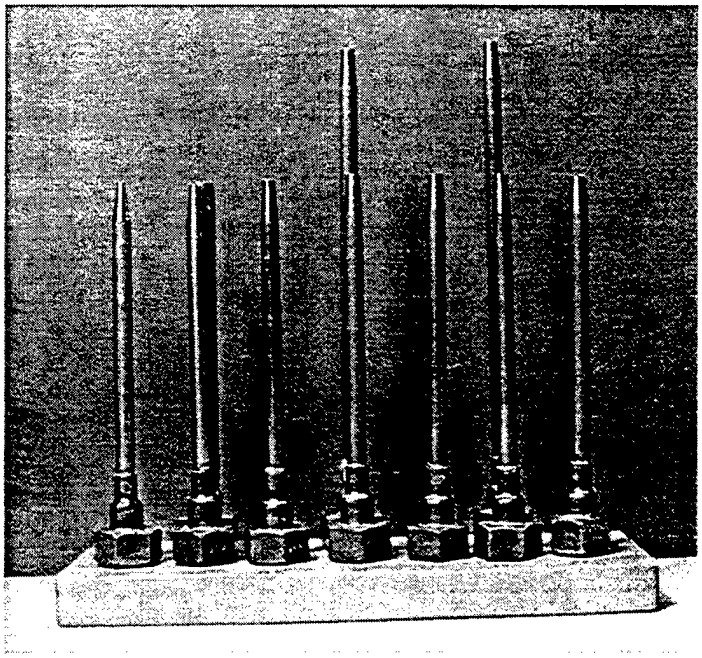

Figure III.13. Four and six-inch length nozzle assemblies of varying diameters.

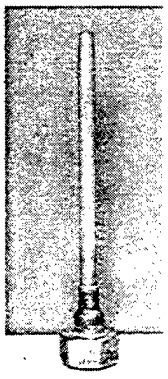

Figure III.14. Four-inch length nozzle assembly of 0.181" diameter.

	Nozzle 1	Nozzle 2	Nozzle 3	Nozzle 4	Nozzle 5
Tube Length (±.05")	4.0"	4.0"	6.0"	4.0"	4.0"
Overall length (±.05")	4.9"	4.9"	6.9"	4.9"	4.9"
Inner diameter (±.0005")	00.090"	00.130"	00.130"	00.152"	0.180"

	Nozzle 6	Nozzle 7	Nozzle 8	Nozzle 9	Nozzle 10
Tube Length (±.05")	6.0"	4.0"	4.0"	6.0"	4.0"
Overall length (±.05")	6.9"	4.9"	4.9"	6.9"	4.9"
Inner diameter (±.0005")	0.180"	00.181"	0.182"	0.182"	0.190"

Table III.1. Nozzle assemblies manufactured.

G. TANK

The water column is bounded by a right-cylindrical acrylic tube. Its wall thickness is $^1/_8$" and its height 4 *ft*. The acrylic tube fits onto a grooved, *PVC* disk that serves as the rigid foundation. Silicone rubber adhesive sealant bonds the acrylic tube to the *PVC* disk. A rubber O-ring reinforces the watertight seal between inner tube wall and *PVC* disk edge. The disk contains a centered

opening for the *1/2" x 13-thread per inch (coarse)* brass bolt and an offset opening for a drain valve. The tube holds approximately 22 *gals* of water in approximately 5137 in^3 of volume. The 22 *gals* of water exert a force of approximately 187 *lbs* onto the *PVC* disk, which has approximately 108 in^2 of surface area in contact with the water. The water column thus exerts just over 1.7 *psi* of hydrostatic pressure onto the *PVC* disk.

H. PRESSURE RESERVOIR

The pressure reservoir maintains a ready volume of nitrogen in linear combination with the solenoid valve and nozzle assembly. It is a steel cylinder of approximately 12" height and 5" diameter, with hemispherical ends. Its capacity is approximately 200 in^3 (3.5 *l*) of nitrogen gas pressurized to 1-17 *psi*. At the 1" diameter opening in one end, a coupler connects the pressure reservoir, input from its dedicated pressure regulator, and output to the solenoid valve.

The base source of pressurized nitrogen is a nitrogen bottle nominally charged to between 1500-2000 *psi*. Because of its size, it is located some distance away from the apparatus. Approximately 4 *ft* of flexible tubing connect the nitrogen bottle to the apparatus.

The pressure reservoir and attached pressure regulator are essential to smooth system operation. Without these, a direct connection between nitrogen bottle and solenoid valve adversely affects performance. Tubing length and bends cause excess wall friction and pressure losses in the supply nitrogen.

Section IV.I describes apparatus performance using a pressure reservoir versus using a direct line between the nitrogen bottle and solenoid valve. In addition to the experimental results found in Section IV.I, if the 1500-2000 *psi* nitrogen bottle is directly attached to the solenoid valve, two problems immediately arise:

- The pressure regulator attached to the 1500-2000 *psi* nitrogen bottle is not precise enough to measure the 1-17 *psi* input to the nozzle assembly. Its gauge is graduated at 2 *psi* increments. The following pressure regulator has a more precise gauge that is adjacent to the pressure reservoir.

- If the nitrogen bottle pressure regulator output is adjusted between nitrogen bursts, an excessive burst of nitrogen blows through the nozzle as the system adjusts. This phenomenon does not occur when the pressure reservoir is used because its ready supply of pressurized nitrogen stabilizes the system when the supply pressure changes.

Although minor, an additional observation occurs when the nitrogen supply is cut off at the nitrogen bottle pressure regulator output. In this case, the system has only one remaining shot of pressurized nitrogen available. This final shot of nitrogen is extremely unstable, as system pressure rapidly dissipates in a violent burst of nitrogen through the nozzle. Using the pressure reservoir enables a controlled, gradual loss of pressure over many bursts. In this case, the pressure reservoir maintains smooth operation even after the nitrogen supply is closed.

I. TUBING

All tubing is flexible, reinforced Norprene tubing. Dimensions are .094" wall thickness, $^{7}/_{16}$" outer diameter and $^{1}/_{4}$" inner diameter. Though the apparatus is designed to transport and control nitrogen gas up to 17 *psi*, the tubing carries a 250 *psi* (at 70° *F*) rating for safety.

J. NOZZLE HANDLING TOOL

An innovative component of the apparatus is a non-integrated support tool. The nozzle handling tool was designed and fabricated by Jaksha (Modelmaker, Naval Postgraduate School). This is an extremely useful tool that inserts and removes an individual nozzle assembly from the apparatus. It is similar to an automobile spark plug tool.

Each nozzle assembly is designed to fit snugly into the receptacle tip of the nozzle handling tool. Since the nozzle assembly sits in the lower portion of the water column, it sits almost 4 *ft* out of reach. The nozzle handling tool extends into the tank to solve the problem. Without it, nozzles could not be interchanged, since the *PVC* disk is permanently attached to the acrylic tube.

Technique is critical when interchanging nozzle assemblies. As described in Section III.G, a bolt extends through the center of the *PVC* disk. Figure III.15 shows the arrangement. One bolt end extends into the water to hold a nozzle assembly. The other bolt end extends below the tank and is permanently attached to a luer fitting. The luer fitting allows solenoid valves to be

interchanged. A nut fits around the bolt beneath the *PVC* disk. This nut tightens against a washer and silicone rubber adhesive in contact with the *PVC* disk. Care must be taken not to over-tighten the nozzle assembly onto the bolt. If too much torque is applied, the bolt will turn and loosen the nut. Since the nut will no longer fit flush against the washer and silicone rubber adhesive, water will leak through the *PVC* disk. To protect against leaks after a nozzle assembly is attached or removed, the bolt should be inspected, and tightened if necessary.

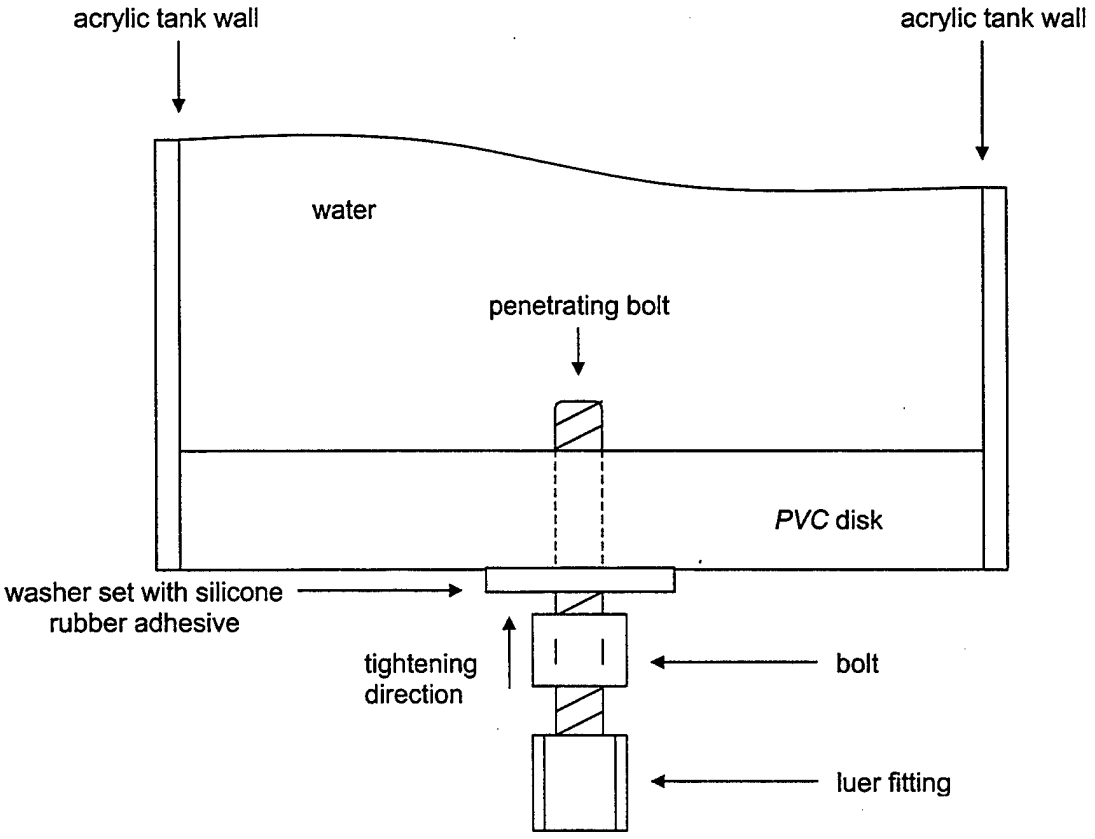

Figure III.15. Cut-away view of *PVC* disk and penetrating bolt.

K. STAND

The stand is essential to apparatus stability. It is constructed of heavy-gage metal and able to support the 187 *lbs* of water plus associated parts. The acrylic tube, *PVC* disk and water column are fitted onto a $^{3}/_{4}$" plywood square that is screwed onto the top of the metal stand. For durability, the metal stand is primed and coated with rust-resistant paint. The wood surfaces are coated with clear polyurethane for water resistance. Heavy-duty wheels allow easy movement when filled.

IV. EXPERIMENT

Experimentation began with the objective of routinely producing toroidal bubbles. Once this was accomplished, nitrogen bursts using many different initial conditions were observed. Many interesting phenomena appeared during experimentation, such as the interaction of a toroidal bubble with the surface, and how different solenoid valves affect toroidal bubble production rate. Observations in all cases reinforced vortex ring theory, discussed in Chapter II. Observations also exhibited the stochastic nature of toroidal bubble formation.

A. HYDROSTATIC PRESSURE

The pressure that the water column exerts upon each nozzle tip is ρgh, where ρ is the density of water, g is the acceleration due to gravity, and h is the vertical distance from the water surface to the tip of the nozzle. The height of the water is approximately 47". The water column thus exerts 1.7 *psi* of hydrostatic pressure onto the *PVC* base. The 4" nozzle tip rests 4" from the bottom of the water column, therefore extending $^{1}/_{12}$ of the total water column height. Since hydrostatic pressure linearly increases with depth (water column height), the 1.7 *psi* total hydrostatic pressure is multiplied by $^{11}/_{12}$ to find the local hydrostatic pressure at the 4" nozzle tip, yielding 1.56 *psi*. Calculated in the same manner as for the 4" nozzle tip, hydrostatic pressure at the 6" nozzle tip is

1.49 *psi*. Bubbles are only expected to occur if the reservoir pressure exceeds the hydrostatic pressure at the nozzle tip; this was experimentally confirmed.

B. NOZZLE AND SOLENOID SELECTION

Nozzle assemblies of length 4" and 6" were manufactured. These lengths placed the nozzle tip well into the water column to avoid possible bottom effects on toroidal bubble formation. It was initially unclear whether the toroidal bubble would form above the nozzle tip or along the outer walls of the nozzle tube. The latter can occur, for example, when a smoke ring is created. However, this is unlikely in our case because a toroid forms from a large initial bubble that is produced above the nozzle tip.

Experimentation showed the toroidal bubble formation to be independent of bottom effects. Since a toroidal bubble forms above the nozzle tip, the bottom boundary visually had no effect. For both 4" and 6" nozzle lengths, toroidal bubbles formed clear of the bottom. As a result, only one nozzle length was needed for further experimentation. The 4" length nozzle was selected instead of the 6" length nozzle because it forms a toroidal bubble lower in the water column, increasing rise time and observation opportunities.

The Burkert solenoid valve (pictured in Figure III.4; see Section III.E for valve specifications) was tested first. The 0.090", 0.130", 0.152" and 0.181" diameter nozzle assemblies were tested at 2 *psi*, 4 *psi*, 6 *psi*, 8 *psi*, 10 *psi*, 12 *psi* and 14 *psi* nitrogen input pressures. The tubing length between the pressure reservoir and solenoid valve was set at 7.50". 50 bursts of nitrogen were

observed for each combination of nozzle assembly and pressure. For this first round of trials, 1400 nitrogen bursts were thus observed.

The second round of trials also used the Burkert solenoid valve. All parameters remained constant except the tubing length between pressure reservoir and solenoid valve. For this round of trials, the length was reduced from 7.50" to 1.75", a 77 percent reduction. The purpose was to determine the effects that wall friction had on nitrogen flow between the pressure reservoir and solenoid valve. Again, 1400 bursts were observed.

The following symbols were used to qualitatively evaluate each nitrogen burst:

- ● one toroidal bubble generated; excellent shape; reaches the top surface intact
- ○ one toroidal bubble generated; degenerative; does not reach the top surface intact
- ●○ two toroidal bubbles generated; excellent shape; one toroidal bubble reaches the top surface intact
- ○○ two toroidal bubbles generated; degenerative; do not reach the top surface intact
- x no toroidal bubble generated

Tables IV.1 and IV.2 display the results for each round of 1400 nitrogen bursts using the different tubing lengths.

1.75" Length of Tubing Between Pressure Reservoir and Burkert Solenoid Valve		
Result	Occurrences	Percentage (1400 trials)
•	393	28
o	702	50
•o	12	1
oo	52	4
x	241	17
Number of pressure/nozzle combinations that yield at least 40 percent • occurrences: 4		

Table IV.1. Qualitative results from 1400 nitrogen bursts using 1.75" length of tubing and Burkert solenoid valve.

7.50" Length of Tubing Between Pressure Reservoir and Burkert Solenoid Valve		
Result	Occurrences	Percentage (1400 trials)
•	367	26
○	722	52
•○	13	1
○○	49	3
x	249	18
Number of pressure/nozzle combinations that yield at least 40 percent • occurrences: 6		

Table IV.2. Qualitative results from 1400 nitrogen bursts using 7.50" length of tubing and Burkert solenoid valve.

Tables IV.1 and IV.2 clearly show that tubing length between the pressure reservoir and solenoid valve has minimal effect on toroidal bubble formation. The results are almost identical. Even so, the decision was made to continue testing with the 1.75" tubing only. This tubing length yielded slightly more •, approximately the same •○, and slightly less x occurrences.

The third round of trials used the Skinner solenoid valve (see Section III.E for valve specifications) and 1.75" tubing between pressure reservoir and solenoid valve. The same symbols are used to qualitatively evaluate each nitrogen burst. Table IV.3 shows the results.

1.75" Length of Tubing Between Pressure Reservoir and Skinner Solenoid Valve		
Result	Occurrences	Percentage (1400 trials)
•	543	39
o	499	36
•o	2	0
oo	16	1
x	340	24
Number of pressure/nozzle combinations that yield at least 40 percent • occurrences: 14		

Table IV.3. Qualitative results from 1400 nitrogen bursts using 1.75" length of tubing and Skinner solenoid valve.

Appendices A and B are a diary of trials for each pressure-nozzle-solenoid combination using the 1.75" tubing connection between pressure reservoir and solenoid valve. Since no further work with the 7.5" tubing connection was done, the 7.5" results are not included.

To ensure an unbiased comparison between the Burkert and Skinner solenoid valves using the 1.75" tubing, the following electrical settings were used for all trials:

- 50 *Hz* signal frequency (function generator output to power supply amplifier; yields 0.01 *s* solenoid valve nominal open time)
- 100 *mHz* burst rate (function generator output to power supply amplifier; yields 10 *s* between successive nitrogen bursts)
- 10 V_{pp} amplitude (function generator output to power supply amplifier)
- 55 V_{pp} amplified amplitude (power supply amplifier output to solenoid valve; sufficiently above solenoid threshold voltage corresponding to 50 *Hz* signal frequency)

Table IV.4 displays the five optimum combinations of pressure, 4" nozzle assembly and solenoid valve at the 1.75" tubing connection length. Fifty nitrogen bursts were observed for each nozzle assembly.

Inner diameter (±.0005")	00.181"	00.181"	00.181"	00.181"	00.130"
Pressure Reservoir	2 *psi*	2 *psi*	6 *psi*	4 *psi*	4 *psi*
Solenoid Valve	Skinner	Burkert	Skinner	Skinner	Skinner
Symbolic Result and Percent Occurrence	• 94 %	• 78 %	• 78 %	• 64 %	• 60 %

Table IV.4. Top five qualitative results from all combinations tested.

The 0.181" diameter nozzle assembly in combination with 2-6 *psi* nitrogen bursts yields optimal results. The Skinner solenoid valve significantly out-performs the Burkert solenoid valve in the category of consistent, predictable toroidal bubble generation. This may be due to a weaker spring in the Burkert

valve, because its voltage rating (24 V_{DC}) is substantially less than that (120 V_{AC}) of the Skinner valve. A weaker spring would increase the closing time of the valve, and may thus create a more vertically elongated initial bubble, which would be less likely to evolve into a toroidal bubble.

The 0.181" diameter nozzle assembly, 1.75" tube connection and Skinner solenoid valve were selected for further analysis and experimentation. This combination of hardware was predicted to yield the most fruitful results. The 0.090" diameter nozzle assembly, though a relatively poor performer in these initial tests, was also selected. This nozzle was selected to test the effects of small nozzle diameter on toroidal bubble production.

C. STOCHASTIC BEHAVIOR

Each table in Appendices A and B chronicles 50 nitrogen bursts at a specific combination of pressure, solenoid valve and nozzle assembly. Prior to tabulating the results shown in each table, the raw data were analyzed. The results confirmed the comment on stochasticity made in Chapter I; the behavior simply did not follow a predictable sequence, but could be very different from one burst to the next. Figures IV.1 and IV.2 show this variation. Toroidal bubbles did, however, form at a certain percentage rate. Additional testing showed the uncertainty of the formation percentage rate to be ± 10 percent for 20 trials.

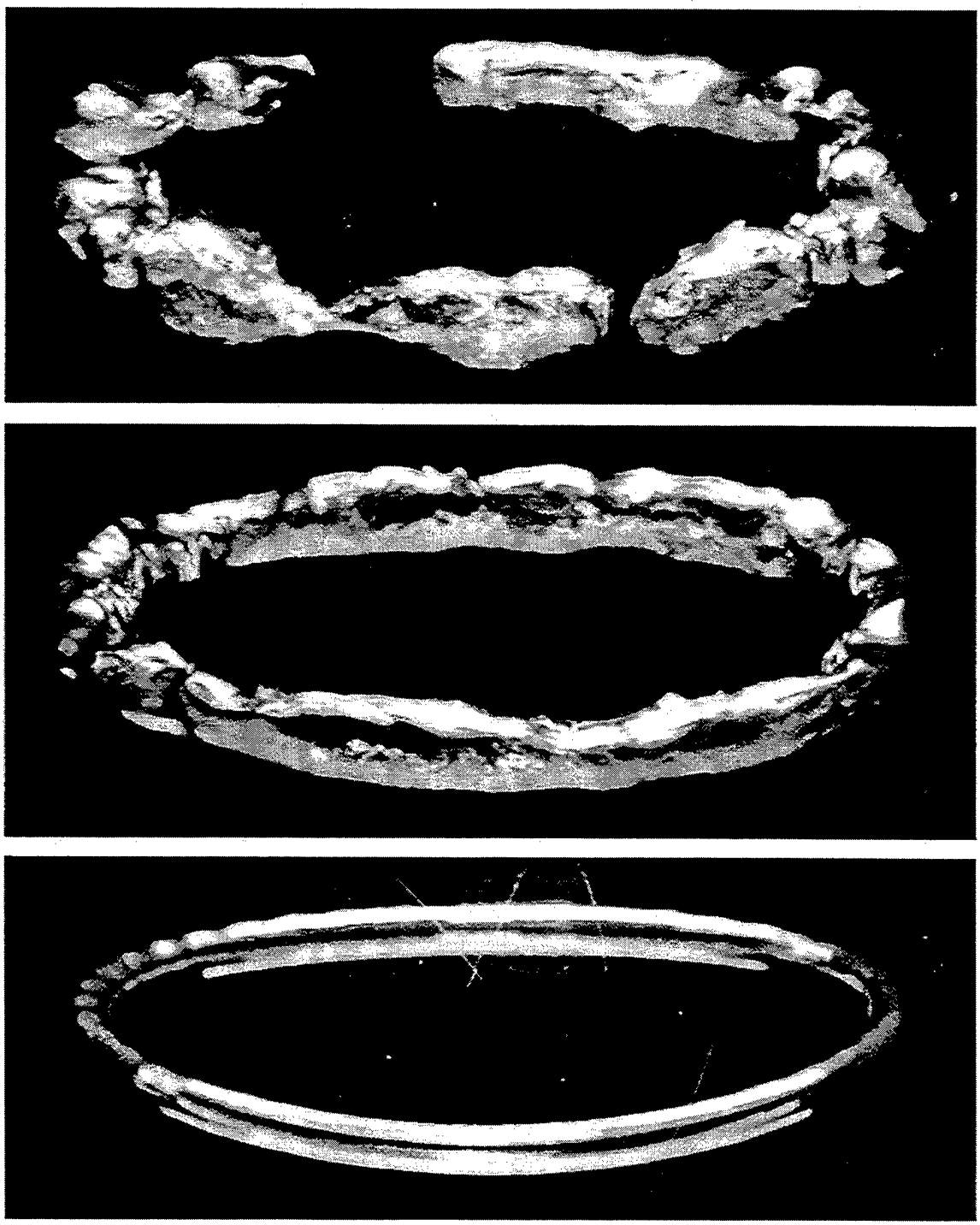

Figure IV.1. Broken, rough and smooth toroidal bubbles.

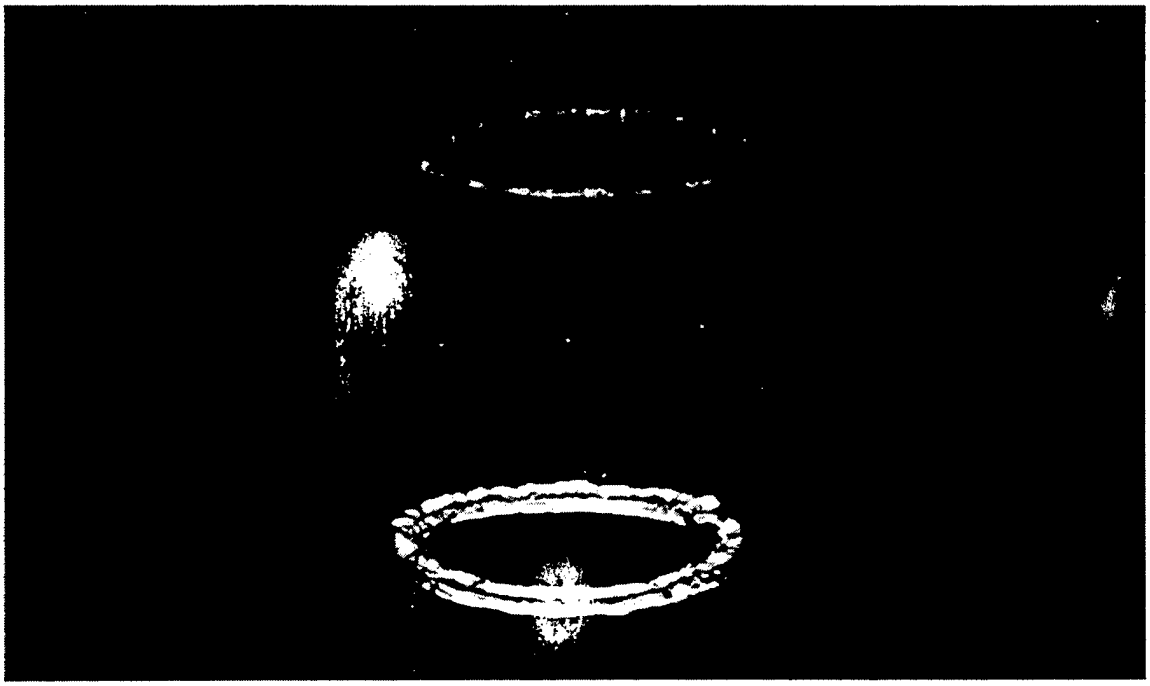

Figure IV.2. Rising toroidal bubble with upper reflection in the acrylic tank.

D. OBSERVATIONS FROM SURROUNDING LIQUID

Water column observation details much about toroidal bubble formation and behavior. Small, trailing, spherical bubbles regularly form above the nozzle tip after each nitrogen burst. This is particularly true when the nitrogen pressure exceeds 8 *psi*. Section IV.G details some ideal pressures to form a toroidal bubble; any pressures above these will cause excess nitrogen to reside in the water column. There were no observations of a single spherical bubble forming above a toroidal bubble, in contradiction to some numerical simulations.

A smooth toroidal bubble, when formed, travels quickly to the surface relative to these residual nitrogen bubbles. After the toroidal bubble forms and rises, the residual bubbles show vertical movement only; they slowly rise to the surface due to their buoyancy. This observation indicates that a toroidal bubble does not cause currents to form in the water column after it passes. The residual bubbles do not swirl above the nozzle tip. This lack of movement in residual bubbles indicates an unimpeded field, free of excessive currents, in which a toroidal bubble forms and rises.

A great deal of excess nitrogen resides in the water column following nitrogen bursts above 10 *psi*. This excess nitrogen rises to the surface just below the toroidal bubble. As described in Chapter II, the toroidal bubble flow rotates about the vortex core. The velocity in the interior of the ring is in the direction of overall movement, and is perpendicular to the toroidal bubble plane. The rotation creates a lower pressure in the plane. As visually observed, this

draws in the excess nitrogen and propels it through the top of the toroidal bubble. Because of this effect, the excess nitrogen often bursts through the surface ahead of the toroidal bubble. As detailed in Table IV.3, some nitrogen bursts generate two toroidal bubbles. The lower pressure in the plane of the first toroidal bubble sometimes draws the lower toroidal bubble through it. This phenomenon is known as the "leapfrog" effect. For all observations of two toroid bursts, this action resulted in the lower toroidal bubble dissipating as it leap-frogged through the upper.

E. INTERACTION WITH SURFACE

Toroidal bubble interaction with the surface is an interesting aspect of the experiment. At pressures below 8 *psi*, most toroidal bubbles produced are thin. A thin toroidal bubble has a relatively small axial diameter in relation to its overall radial diameter. At pressures 8 *psi* and above, a toroidal bubble forms with a relatively large axial diameter. The internal circulation around the vortex ring becomes visibly faster and stronger.

The top surface destroys toroidal bubbles regardless of vortex shape or strength. Two visible effects occur when a toroidal bubble is destroyed: the water column surface is altered, and the toroidal bubble disintegrates into a random array of smaller bubbles.

A toroidal bubble generated below 8 *psi* has little physical effect on the surface. The toroid-surface interaction produces some local surface displacement, but damping quickly restores the surface to near equilibrium. In

contrast, a toroidal bubble generated at 8 *psi* or above has a clear effect on the surface. The fluid in our toroidal bubble rotates from bottom to top, through the middle of the ring, in the direction of upward movement. This is axial flow in the direction of propagation. When a toroidal bubble reaches the surface, the axial flow causes the surface to rise in the center of the dissipating ring. A toroidal bubble becomes much stronger as nitrogen pressure increases. A stronger toroidal bubble interacts violently with the surface. Eventually, the rising action on the surface becomes a plume of water. These plumes occur at 12 *psi* and above. Many times, the water plume sprayed the areas surrounding the acrylic tank.

Toroidal bubble interaction with the surface also affects the water column. As some toroidal bubble energy is dissipated in surface waves, the remainder is lost to formation break-up. As a toroidal bubble reaches the surface, the smooth ring breaks apart into smaller bubbles. These bubbles burst downward into the water column against the original direction of toroidal bubble movement.

F. SOLENOID VOLTAGE SIGNAL

Experimentation yielded an interesting, corollary relationship between signal frequency and threshold voltage required to operate the solenoid valve. Threshold voltage is defined as that voltage required to cause the metal plunger to impact the top of the casing, indicating a fully open position. As shown by Figure IV.3, the threshold voltage varies approximately linearly with signal frequency, which is inversely proportional to solenoid valve open time. Hence,

the threshold voltage varies inversely with the solenoid valve open time.

The cause of this phenomenon is the magnetic field created by the electromagnetic coil. When signal frequency is low, the solenoid valve is held open for a discernible amount of time. This delay between opening and closing actions allows the lower threshold voltage to build up a magnetic field to move the plunger. When signal frequency is high, the solenoid valve is held open for a short time. There is little delay between opening and closing actions to allow the magnetic field to build in the coil. As a result, the threshold voltage must be higher, and may now be considered an electrical impulse. As described in Sections III.B and III.D, the power supply amplifier may be operated with a single channel output or bridged output. Though a relatively high threshold voltage is required to open the solenoid valve with a high input signal frequency, the single channel output is sufficient.

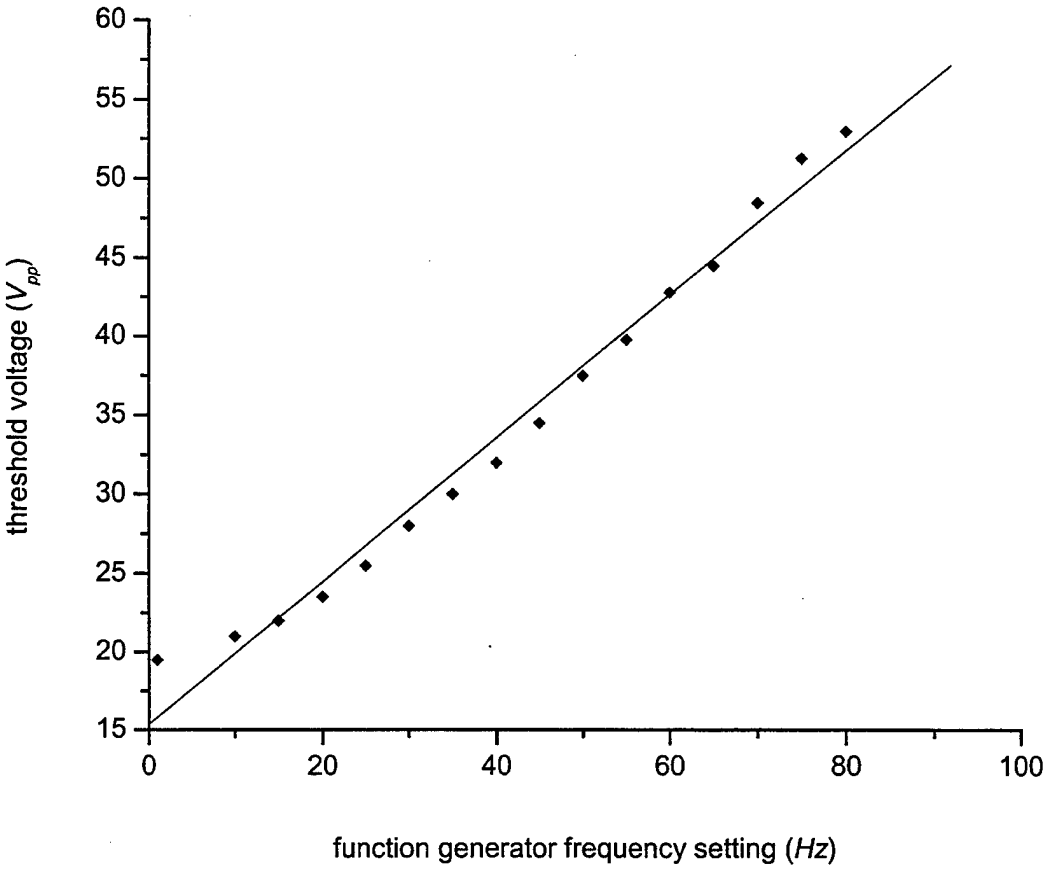

Figure IV.3. Relationship between threshold voltage to solenoid, and rectangular wave input frequency.

G. DRIVE PLANE PORTRAITS

Of great importance to toroidal bubble formation is the combination of pressure and burst length. These drive parameters create the conditions for which a toroidal bubble can be produced. As discussed in Chapter III, pressure is regulated at the pressure reservoir and burst length is regulated at the function generator. The amplified signal from the function generator drives the solenoid

valve to open and close. The temporal duration of this signal is known as the solenoid valve on-time (the time that the solenoid valve has an electrical input). For our rectangular wave input, Section III.A describes the relationship between the function generator setting in *Hz* and the on-time in *s*.

Figure IV.4 shows a frequency-pressure drive plane for the 0.181" nozzle assembly. Because the 0.181" nozzle assembly is the best performer of the 10 nozzles manufactured (see Figure III.14 and Section IV.B), 40 and 80 percent formation thresholds were selected. This plot shows a frequency-pressure region where a toroidal bubble is most likely to occur. Each point represents 20 trials, each separated by 10 seconds. The stochastic nature of the production of toroidal bubbles is dramatically evidenced by the lack of clear, smooth boundaries between the regions corresponding to 0-39%, 40-79% and 80-100%. Many more trials would be required for such boundaries to become clearly defined. The optimum setting for the 0.181" nozzle assembly is 70 *Hz* (.029 *s*) / 3 *psi*, for which 19 toroidal bubbles formed from 20 nitrogen bursts.

Figure IV.5 shows the number of pressure settings for which a frequency achieved a 40 percent toroidal bubble formation rate. Pressure settings range from 1-11 *psi* in 1 *psi* increments. Toroidal bubbles form at a less than 40 percent rate from 1.7 – 2 *psi* and above 10 *psi*. Below 1.7 psi (hydrostatic pressure at the 4" length nozzle tip, as calculated in Section IV.A), no toroidal bubbles will form. From this histogram, the optimum input signal is 60 *Hz* (though the setting of 70 *Hz* (.029 *s*) / 3 *psi* yielded the highest singular

percentage). Figure IV.6 shows the number of pressure settings at which the same frequencies achieved an 80 percent formation rate. From this histogram, the optimum input signals are in the range 40-70 *Hz*.

Figure IV.7 shows a frequency-pressure drive plane for the 0.090" nozzle assembly. Because the 0.090" diameter nozzle assembly is the worst performer of the 10 nozzles manufactured (see Section IV.B), 20 and 40 percent formation thresholds were selected. The region of toroidal bubble formation is denser than the 0.181" diameter nozzle because the threshold of formation rates is lower (20 / 40 percent vice 40 / 80 percent). The optimum setting for the 0.090" diameter nozzle assembly is 80 *Hz* (.025 *s*) / 3 *psi*, at which 9 toroidal bubble formed from 20 nitrogen bursts, which is significantly lower than for the 0.181" diameter nozzle assembly.

Figure IV.8 shows the number of pressure settings at which a frequency achieved a 20 percent toroidal bubble formation rate. Pressure settings range from 1-17 *psi* in 1 *psi* increments. Toroidal bubbles form at a less than 20 percent rate below 3 *psi* and above 16 *psi*. This pressure range is larger than the 1-11 *psi* range for the 0.181" diameter nozzle assembly because the 20 percent threshold is used. From this histogram, the optimum input signal is 70 *Hz*. Figure IV.9 shows the number of pressure settings at which the same frequencies achieved a 40 percent formation rate. From this histogram, the optimum input signal is 80 *Hz*.

Finally, to give another representation of the trial results, Figures IV.10 and IV.11 give the raw data for the 0.181" and 0.090" diameter nozzles,

respectively. The numerical data field in each plot shows the number of smooth toroidal bubbles produced from 20 nitrogen bursts at each pressure-frequency setting. The previous figures, Figures IV.4 – IV.11, are derived from these raw data fields.

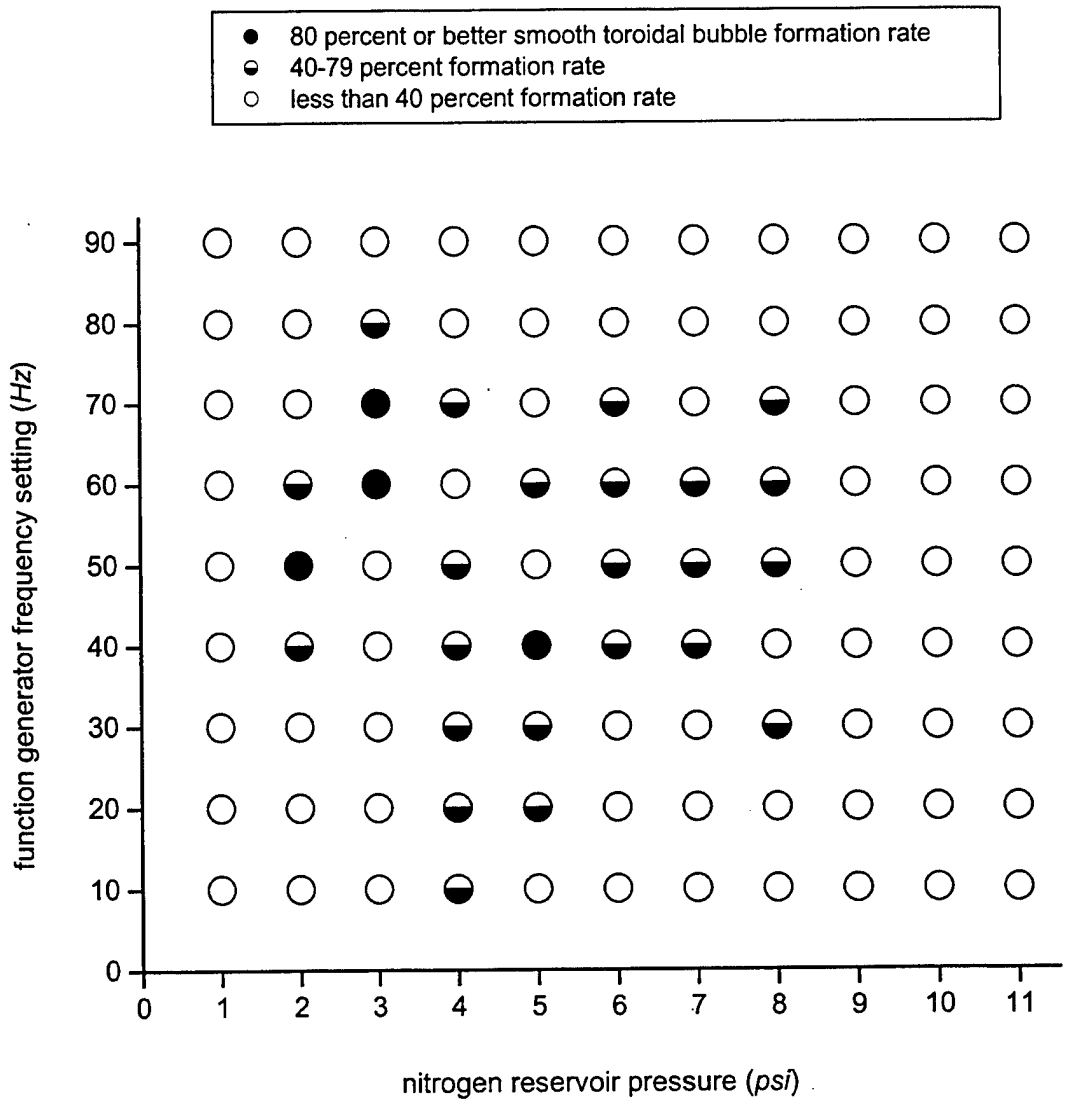

Figure IV.4. Drive plane parameters (solenoid valve on-time, nitrogen pressure) for 0.181" nozzle assembly. Each data point on the plot represents the percent of smooth toroidal bubbles formed from 20 bursts of nitrogen.

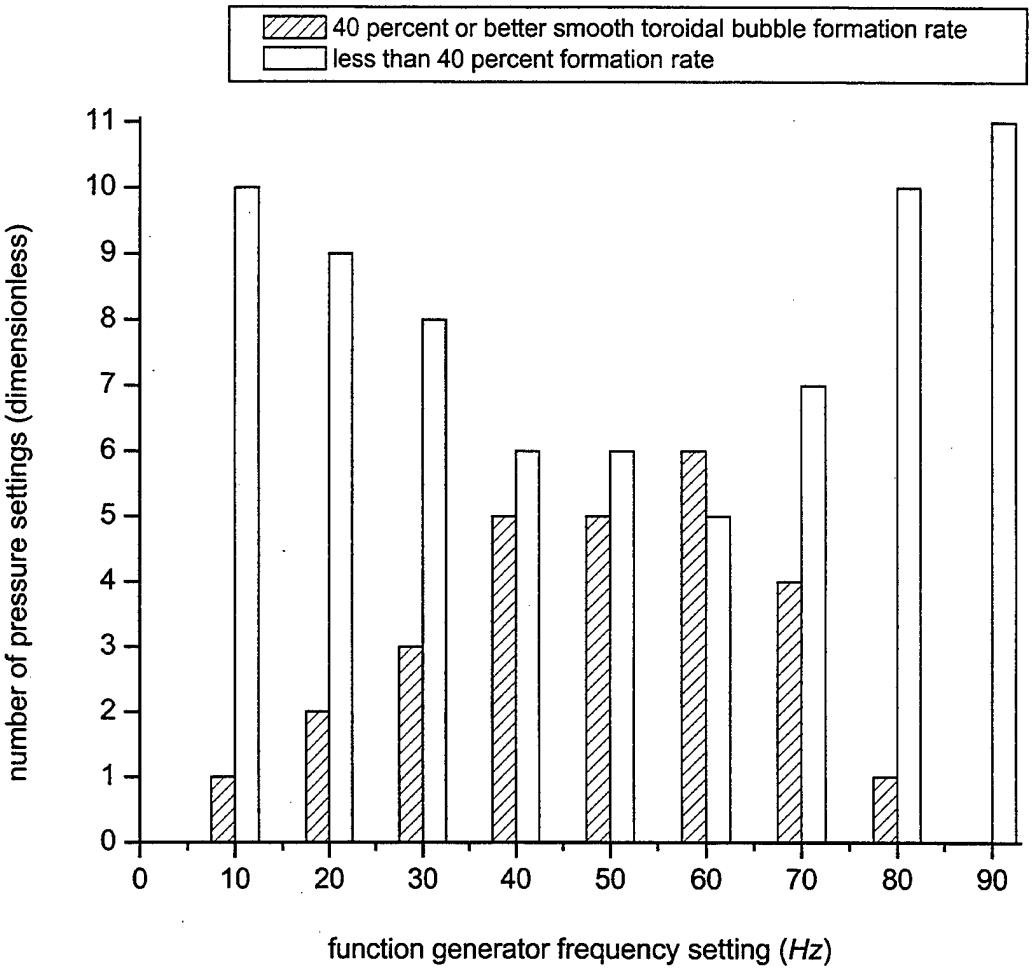

Figure IV.5. Forty percent formation rate for 0.181" nozzle assembly. This plot gives the number of pressures where smooth toroidal bubbles formed at 40 percent rate or better. The pressure range is 1-11 *psi* in 1 *psi* increments.

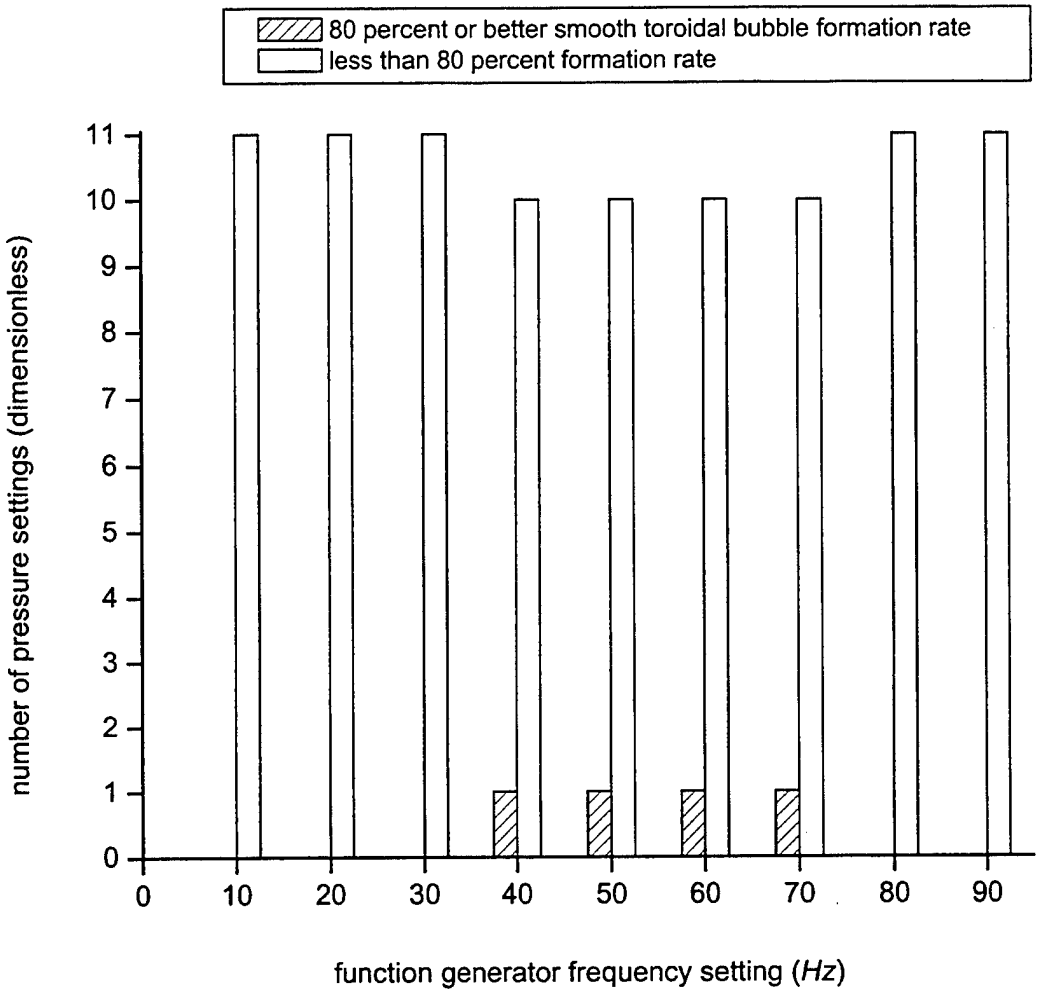

Figure IV.6. Eighty percent formation rate for 0.181" nozzle assembly. This plot gives the number of pressures where smooth toroidal bubbles formed at 80 percent rate or better. The pressure range is 1-11 *psi* in 1 *psi* increments.

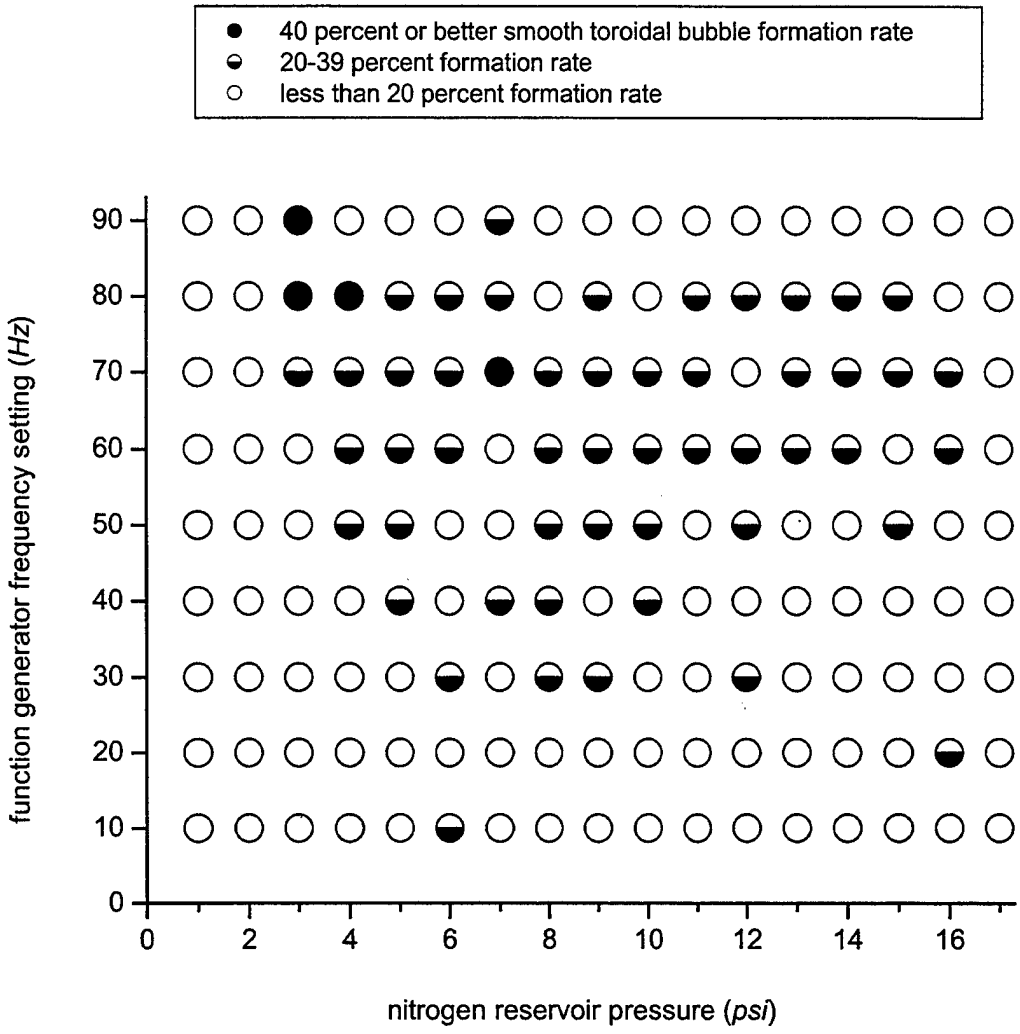

Figure IV.7. Drive plane parameters (solenoid valve on-time, nitrogen pressure) for 0.090" nozzle assembly. Each data point on the plot represents the percent of smooth toroidal bubbles formed from 20 bursts of nitrogen.

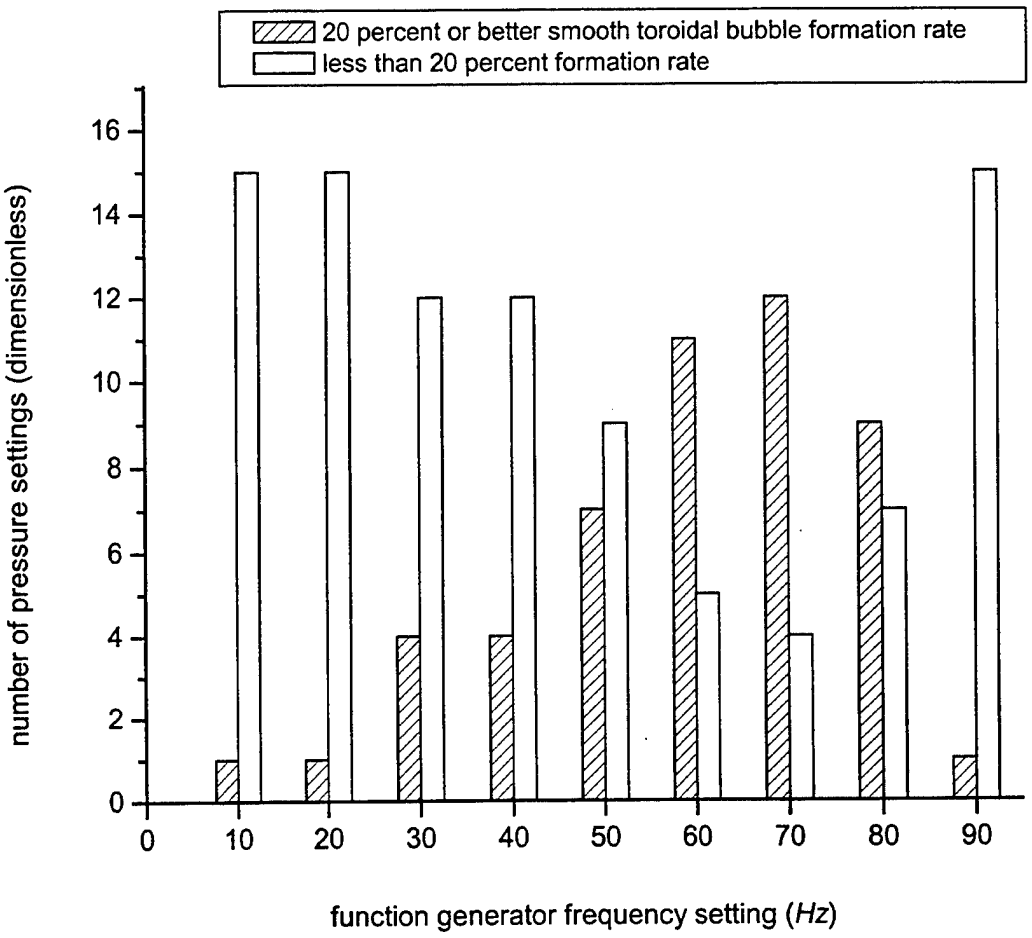

Figure IV.8. Twenty percent formation rate for 0.090" nozzle assembly. This plot gives the number of pressures where smooth toroidal bubbles formed at 20 percent rate or better. The pressure range is 1-17 *psi* in 1 *psi* increments.

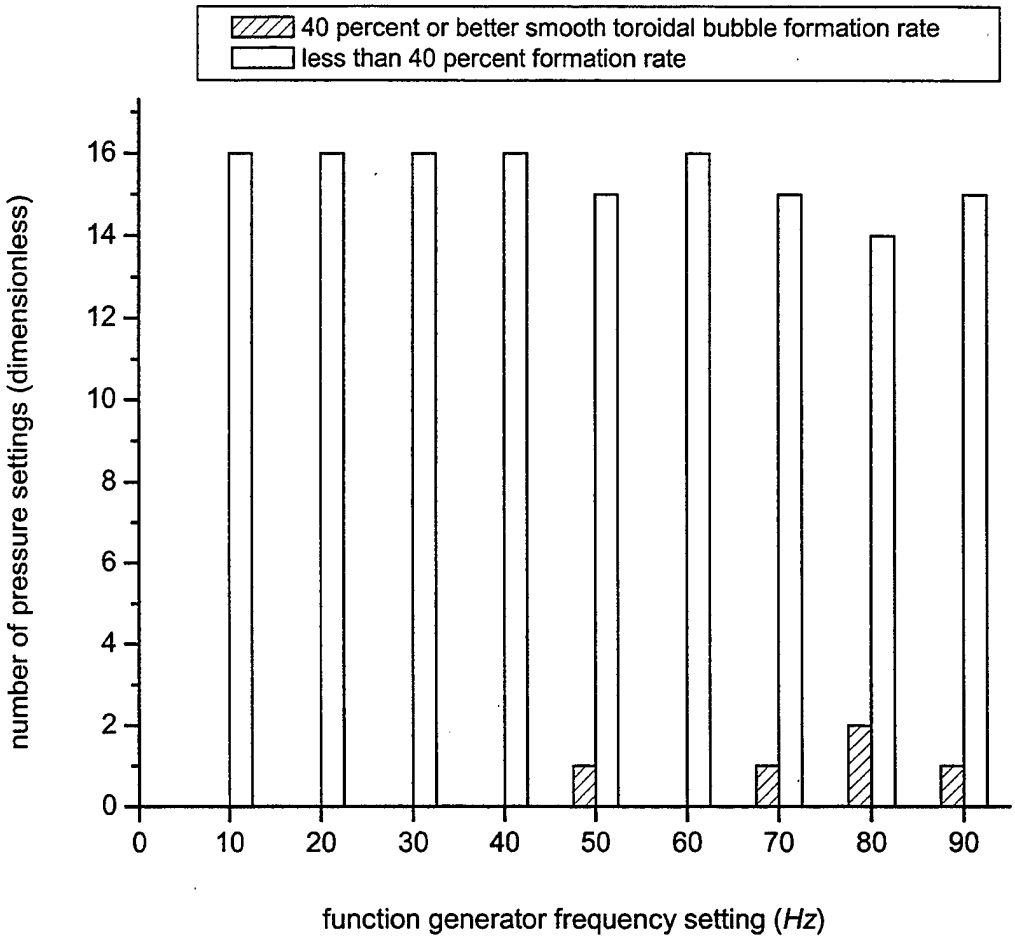

Figure IV.9. Forty percent formation rate for 0.090" nozzle assembly. This plot gives the number of pressures where smooth toroidal bubbles formed at 40 percent rate or better. The pressure range is 1-17 *psi* in 1 *psi* increments.

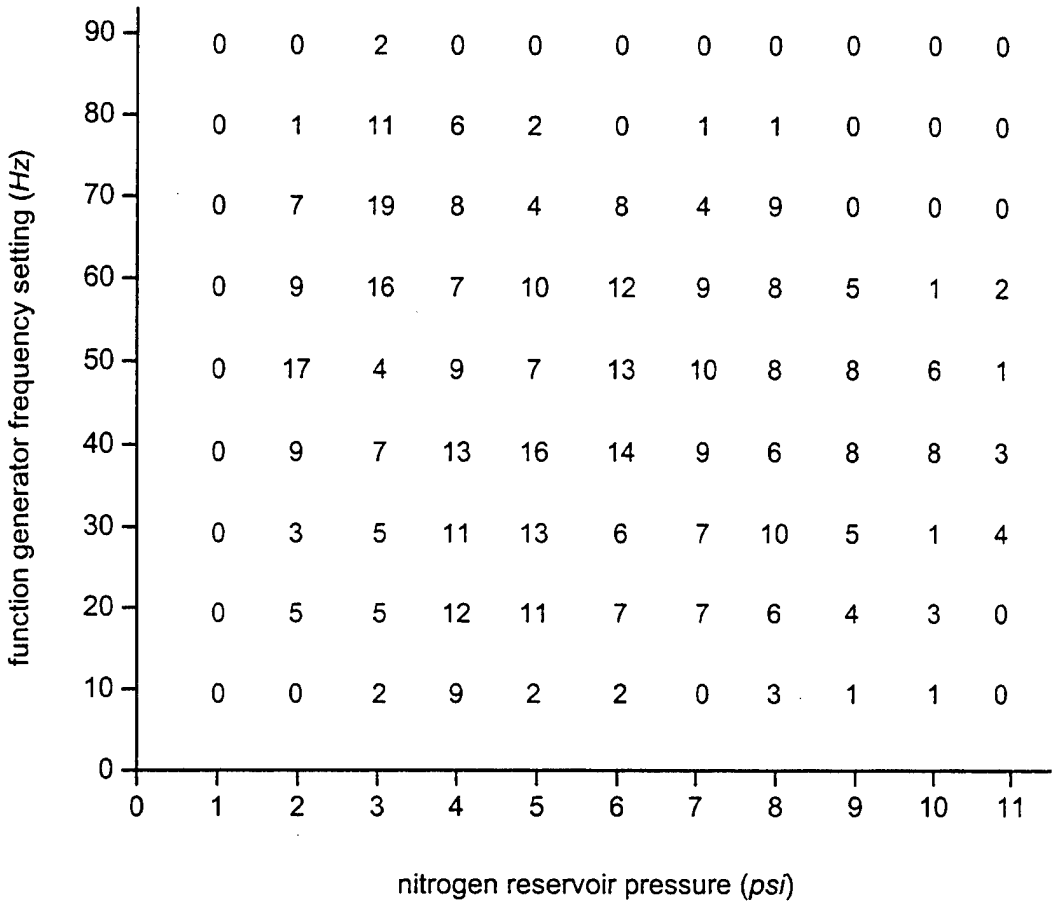

Figure IV.10. Numerical data field for 0.181" nozzle assembly. Each entry in the data field represents the number of smooth toroidal bubbles formed from 20 bursts of nitrogen.

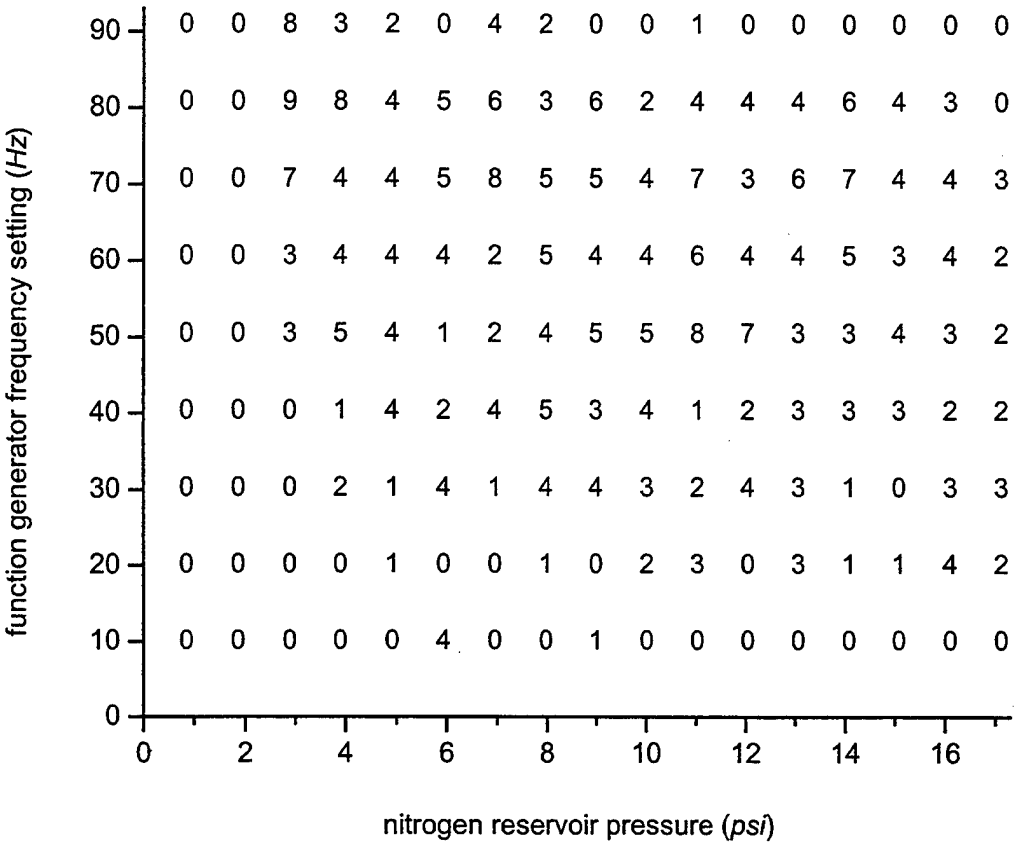

Figure IV.11. Numerical data field for 0.090" nozzle assembly. Each entry in the data field represents the number of smooth toroidal bubbles formed from 20 bursts of nitrogen.

H. LARGE DIAMETER NOZZLE

Trials using a large diameter nozzle assembly were added so that results could be compared to the 0.090" and 0.181" diameter nozzle assemblies. The large diameter nozzle assembly has the same inner diameter, 0.300", as the penetrating bolt through the *PVC* disk (see Figure III.15), allowing comparatively unrestricted nitrogen flow between the solenoid valve output and nozzle tip. The area of the 0.300" diameter nozzle opening is .0707 in^2, compared to .0064 in^2 and .0257 in^2 for the 0.090" and 0.181" diameter nozzles, respectively. The area of the 0.300" diameter nozzle is approximately 11 times the area of the 0.090" diameter nozzle and almost 3 times the area of the 0.181" diameter nozzle.

The 0.300" diameter nozzle assembly was tested using the same independent parameter ranges as for the 0.090" and 0.181" diameter nozzles. Details of these independent parameters are given in Section IV.G. No combination of parameters yielded a toroidal bubble.

There were significant performance differences between the 0.300" diameter nozzle and the smaller diameter nozzles. Unlike the 0.090" and 0.181" diameter nozzles, water filled the 0.300" diameter nozzle after each nitrogen burst. This was evidenced by a steady progression of spherical bubbles from the nozzle tip as water methodically displaced the remaining nitrogen. In contrast, the 0.090" and 0.181" diameter nozzles retained a volume of residual nitrogen within the nozzle tube following each burst. This nitrogen remained in equilibrium, held in place by surface tension at the nozzle tip.

The 0.300" diameter nozzle required more nitrogen pressure to produce a visible burst. Very little nitrogen entered the water column below 5 *psi*. In contrast, the minimum pressure threshold for the 0.090" and 0.181" diameter nozzles was approximately 1.5 *psi*. At 5 *psi* and above, nitrogen bursts created a dissipative vortex ring (not a toroidal bubble) composed of the water that had entered the nozzle tube. This water was forced out of the nozzle by the nitrogen burst. The random, small bubbles from the burst moved about the vortex ring, creating a visual image of the flow. At 8 *psi* and above, the water within the nozzle created a visible spray into the water column.

The 0.300" diameter nozzle assembly was also tested with a shorter burst period. Until now, burst rate had been maintained at 10 *s* between successive nitrogen bursts for all prior tests. The shorter burst period, for example 2 *s* between bursts, caused some broken, turbulent toroidal bubbles. However, no smooth toroidal bubbles were produced.

I. PRESSURE RESERVOIR ADVANTAGES

The pressure reservoir is described in Section III.H. To verify the effect of the pressure reservoir on toroidal bubble formation, the apparatus was retested using a direct connection between nitrogen bottle and solenoid valve, though the pressure regulator. The results were compared to toroidal bubble formation rates obtained using the pressure reservoir.

Four trials of 20 bursts were conducted using the 0.181" diameter nozzle, a 40 *Hz* solenoid valve on-time, and 5 *psi* nitrogen input pressure. Of two trials

conducted using the pressure reservoir, 13/20 and 16/20 smooth toroidal bubbles formed, for an average of 14.5/20 = 72.5 percent toroidal bubble formation rate. This percentage compares favorably with the 16/20 occurrences found in Figure IV.10. Of two trials conducted using a direct connection between nitrogen bottle and solenoid valve, 10/20 and 12/20 smooth toroidal bubbles formed, for an average of 11.0/20 = 55.0 percent toroidal bubble formation rate. This lower rate shows the importance of using the pressure reservoir.

Additional trials were conducted using a lower nitrogen input pressure. These trials determined the pressure reservoir usefulness at low pressures. Figure IV.10 shows a successful, low pressure drive plane combination to be a 50 *Hz* solenoid valve on-time coupled with a 2 *psi* nitrogen input pressure. As before, 20 bursts were observed using the 0.181" diameter nozzle. Of two trials conducted using the pressure reservoir, 17/20 and 16/20 toroidal bubbles formed, for an average of 16.5/20 = 82.5 percent toroidal bubble formation rate. This percentage compares favorably with the 17/20 occurrences found in Figure IV.10. Of two trials conducted using a direct connection between nitrogen bottle and solenoid valve, 1/20 and 3/20 toroidal bubbles formed, for an average of 2.0/20 = 10.0 percent toroidal bubble formation rate. This significantly lower rate confirms the essential nature of the pressure reservoir, especially at lower pressures.

J. SOLENOID VALVE ORIFICE SIZE

Another interesting consideration is the impact of orifice size on toroidal bubble formation rates. Two additional solenoid valves were obtained to determine the effect, if any. The first is a replacement for the Skinner Valve Division solenoid valve described in detail in Section III.E. It has the same specifications and power rating, but was manufactured in the year 2000 vice 1979. Apart from a more modern appearance, this valve is designed to the same parameters as the original. Importantly, the orifice size remains the same at $^1/_8$". The second solenoid valve obtained has the same specifications and power rating, but a $^1/_4$" orifice. It was also manufactured in the year 2000.

Following the same pattern of comparison testing as in Section IV.I, four trials of 20 bursts were conducted using the 0.181" diameter nozzle, a 40 *Hz* solenoid valve on-time, and 5 *psi* nitrogen input pressure. Of two trials conducted using the $^1/_8$" orifice, 10/20 and 12/20 smooth toroidal bubbles formed, for an average of 11.0/20 = 55.0 percent toroidal bubble formation rate. This percentage is consistently low compared to the 16/20 occurrences found in Figure IV.10, which shows that the new solenoid valve is not the equivalent of the original. Perhaps the shape of the internal orifice is slightly different. Of two trials conducted using the $^1/_4$" orifice, 5/20 and 3/20 smooth toroidal bubbles formed, for an average of 4.0/20 = 20.0 percent toroidal bubble formation rate. Besides this much lower formation rate than the $^1/_8$" orifice valve, the $^1/_4$" orifice valve produced more turbulent toroidal bubbles that were axially thicker.

Additional trials were conducted to determine the impact of orifice size on low pressure inputs. Figure IV.10 shows a successful, low pressure drive plane combination to be a 50 *Hz* solenoid valve on-time coupled with a 2 *psi* nitrogen input pressure. As before, 20 bursts were observed using the 0.181" diameter nozzle. Of two trials conducted using the $^1/_8$" orifice, 7/20 and 10/20 toroidal bubbles formed, for an average of 8.5/20 = 42.5 percent toroidal bubble formation rate. This percentage is markedly low compared to the 17/20 occurrences found in Figure IV.10. Of two trials conducted using the $^1/_4$" orifice, 1/20 and 3/20 toroidal bubbles formed, for an average of 1.5/20 = 7.5 percent toroidal bubble formation rate. A third round of trials was conducted. These trials determined the impact of orifice size on high pressure inputs. Figure IV.10 shows a successful, high pressure drive plane combination to be a 50 *Hz* solenoid valve on-time coupled with a 9 *psi* nitrogen input pressure. As before, 20 bursts were observed using the 0.181" diameter nozzle. Of two trials conducted using the $^1/_8$" orifice, 8/20 and 7/20 toroidal bubbles formed, for an average of 7.5/20 = 37.5 percent toroidal bubble formation rate. This percentage compares favorably with the 8/20 occurrences found in Figure IV.10. Of two trials conducted using the $^1/_4$" orifice, 1/20 and 1/20 toroidal bubbles formed, for an average of 1.0/20 = 5.0 percent toroidal bubble formation rate. Many turbulent, degenerative, two-toroid bursts occurred.

Increasing the orifice size of the solenoid valve decreases the toroidal bubble formation rate at low (2 *psi*), medium (5 *psi*) and high (9 *psi*) pressures.

Visually, the effect of increasing orifice size is the same as increasing solenoid valve on-time: more nitrogen gas is allowed to stream through the nozzle.

K. ACOUSTIC EMISSION

A toroidal bubble is expected to emit sound into the water column due to one or more modes of oscillation that are excited during the formation process. An attempt was made to measure these sound emissions with a hydrophone. Figure IV.12(a) shows a typical voltage reading from the hydrophone, representing acoustic pressure. From 0.0 – 1.4 *s*, the sinusoidal wave shows the sum of a low frequency wave that visually dominates and decays slowly, and a high frequency wave that distorts the low frequency wave and decays quickly. At 1.4 *s* from origination, the toroidal bubble reaches the surface and bursts, creating the waveform seen from 1.4 – 2.0 *s*. At our setting of 7 psi, this burst is audible to observers.

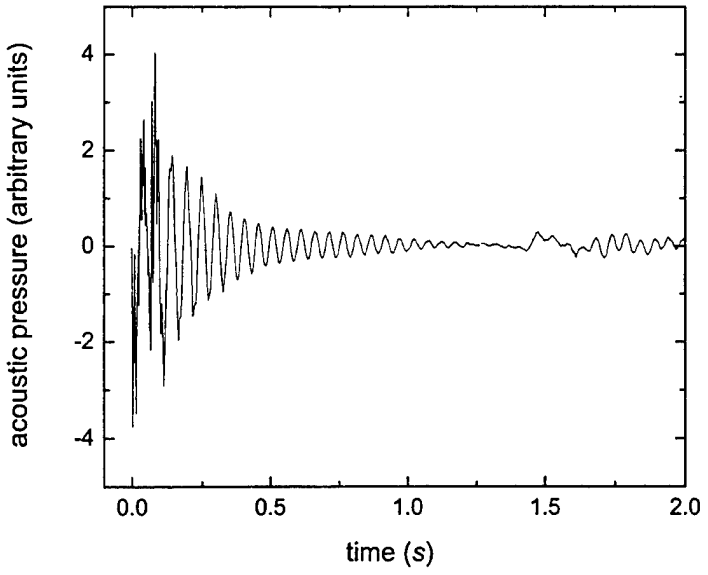

Figure IV.12(a). Acoustic pressure in the water column following a single nitrogen burst. The drive settings are 7 *psi* nitrogen pressure and 30 *Hz* frequency. Clearly shown are: the initial sound as the apparatus generates a toroidal bubble (from 0.0 – 1.4 *s*), and sound emitted after the toroidal bubble strikes the top surface (from 1.4 – 2.0 *s*).

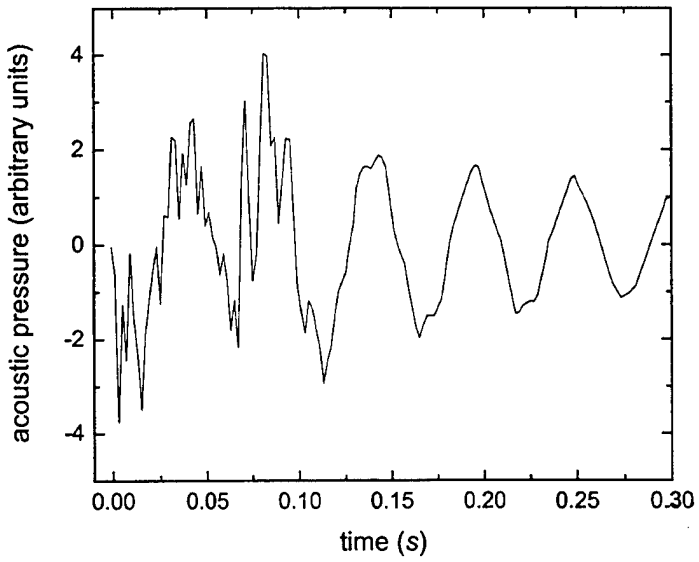

Figure IV.12(b). Beginning of acoustic waveform seen in Figure IV.12(a).

To determine if one or both waveform components originated from the toroidal bubble, two distinct types of nitrogen bursts were compared: those that created a smooth toroidal bubble and those that did not. For both cases, the observed acoustic pressure waveform was similar, indicating that a toroidal bubble did not produce the sound. A likely explanation is that mechanical vibrations of the stand-tank combination, caused by a violent burst of pressurized nitrogen, cause the low frequency acoustic pressure wave. The high frequency signal may be the result of the excitation of an acoustic mode of the water column. Figure IV.12(b) shows the first 0.3 *s* of the observed sinusoidal waveform. From this plot, the high frequency sound clearly distorts the low frequency sinusoidal wave. At about 0.12 *s*, the high frequency sound is no longer evident.

THIS PAGE INTENTIONALLY LEFT BLANK

V. CONCLUSIONS AND FUTURE WORK

This experiment has shown that toroidal bubbles can be routinely generated under controlled conditions. In addition, only slight adjustments made to the apparatus can greatly affect the formation rate. The electrical, mechanical and temporal interactions that produce a toroidal bubble are not trivial.

A. CONCLUSIONS

An apparatus that generates toroidal bubbles has been constructed and tested. Much of the parameter space for the formation of toroidal bubbles has been mapped, and shows a high degree of stochasticity in the formation of toroidal bubbles from a burst of gas. In spite of this, conditions for which there is as much as 90% probability of formation of smooth toroidal bubbles have been found. Previous work by Denardo and Kolaini (University of Mississippi, 1994-1996) yielded only about 40%. A search for acoustic emission of toroidal bubbles has also been conducted, with no positive results.

Upon first inspection, the apparatus seems to be an arbitrary design based on readily available equipment and neatly designed hardware. However, our systematic research clearly shows that any toroidal bubble production system would need a design similar to that described in Chapter III.

Of great importance are the solenoid valve input signal and nitrogen input pressure. The drive plan parameters are detailed in Chapter IV. Since these

parameters are now documented, further research can take place with minimum drive plane experimentation.

A great deal of hardware was needed to build the successful apparatus. From the beginning, we realized that many components would need to be interchangeable. Critical nodes, such as solenoid valves and pressure regulators, needed to be quickly and easily removed and replaced. The luer fittings described in Chapter III worked to perfection. These air-and-watertight fittings are available from Cole-Parmer Instrument Company (distributor information given in Section III.E).

B. FUTURE WORK

1. Formation of a Toroidal Bubble

As mentioned in Chapter I, it is remarkable that a highly turbulent burst of gas into a liquid can lead to the formation of a smooth, highly ordered state of a toroidal bubble. A photograph sequence of the formation could lead to a qualitative understanding of the process. A digital video camera is able to capture such a sequence.

The digital video camera has a limited number of frames per second, typically 30 frames per second in the non-interlaced mode. In a recording session, the digital video camera captures a continuous sequence of single frames, which can then be isolated. This method suffers from the fact that a toroidal bubble is stochastic in nature; it is not the same from one creation to the

next. However, results in Chapter IV show that conditions exist for which nearly identical toroidal bubbles can be created.

Numerous attempts were made to capture the formation of a toroidal bubble in the water column. However, internal reflection proved to be a formidable hindrance to successful image recording. At negative camera angles (looking down on the nozzle tip), a false image occurs above the bubble. At positive camera angles, a false image occurs below the bubble. Figure IV.2 shows this internal reflection. Refraction of external light also causes images to be obscured. A solution to this problem is given below in Subsection V.B.1.

2. Evolution of a Toroidal Bubble

As described in Chapter II, the speed of a toroidal bubble decreases and the ring diameter increases as the toroid travels upward. This behavior occurs because the vortex ring energy increases due to the buoyant force. It should be possible to predict vortex ring speed and diameter as a function of time or height. Experimentally, data could be gathered with a digital video camera with images downloaded to a computer. Meter sticks could be placed as distance rules along the sides, top and bottom of the tank. Simple, approximate corrections would be made due to continually changing camera line-of-sight as the toroidal bubble rises. In general, the camera would not be perpendicular to the toroid, and would be affected by refraction caused by the cylindrical geometry of the tank, as discussed previously in Subsection V.B.1.

The comparison of theory and experiment may show a systematic deviation due to the presence of this cylindrical boundary, which imposes the condition of zero flow velocity perpendicular to the boundary. The effect might be qualitatively understood and perhaps calculated by the method of images. This method may apply because the boundary condition may be met by considering a concentric image toroid outside the tank.

For sequential photography of a rising toroidal bubble, it is beneficial to replace the cylindrical tank with a square one. The tank could be constructed by fusing thick, planar sheets of acrylic (greater thickness is required for strength). This robust tank design is also advantageous for a hands-on display (see Subsection V.B.3, below). The square cross section allows a relatively undistorted view by eliminating refraction. Though ideal for photography and visual display, the square cross section tank makes method of images analysis much more difficult.

Another possible research topic regarding toroidal bubble evolution involves its eventual instability. As the diameter of an initially smooth toroid becomes larger and larger, the toroid eventually breaks into a number of smaller, spherical bubbles. This is most likely due to surface tension. The scientific literature may contain a theoretical linear stability analysis of a toroidal bubble subjected to sinusoidal modulations of its cross-sectional area. An experiment with a digital video camera could be used to gather data on occurrences of the instability. These results could then be compared to theory.

3. Hands-on Apparatus

As stated in Chapter I, an eventual goal of this work is to make a hands-on apparatus that could be used in museums and physics department hallways. The display would allow an observer to adjust gas pressure in the reservoir and pulse on-time to the solenoid valve. Air would replace nitrogen as the injected gas. The air can be supplied by an in-house compressor or compact, dedicated compressor adjacent to the water tank. The observer could use a momentary switch to fire the solenoid valve. Two activations of the momentary switch in rapid succession could produce two toroidal bubbles that undergo the leapfrog interaction described in Chapter IV.

The oscilloscope is not needed for a hands-on apparatus, and it is undesirable to use a high quality, laboratory function generator and power amplifier. For this purpose, a dedicated function generator can be inexpensively constructed from integrated circuits. A solid state relay would switch the output of DC power to the solenoid valve. The DC supply could be built as a simple, filtered rectifier that operates from line power.

The task of building a safe and durable apparatus is a challenging one, particularly if line power, compressed gas and appreciable water volume are used. However, such a project is worthy because it allows the public to directly observe the beauty of stable toroidal bubbles and the richness of the stochastic behavior.

4. Acoustic Emission

Section IV.K details the process for measuring sound in the water column. Of interest is whether or not the sound emitted by a toroidal bubble is detectable. Although no acoustic signal from a toroidal bubble is currently apparent, such a signal may be obscured by the oscillations from the apparatus. A next step could be to attempt to remove these oscillations, if possible. For example, placing heavy weights on the platforms will reduce the low frequency oscillations. Careful analysis of the time record may then yield an acoustic signal from toroidal bubble oscillations. Rough theoretical calculations of the expected frequencies would be useful in this search.

5. Effects of Acoustic Noise

Larraza and Tucholski (2000) have shown theoretically that a spherical bubble in a liquid subjected to homogeneous, isotropic acoustic noise, can experience a drag force. This drag force can be positive or negative, depending upon the noise spectrum shape and bubble resonance frequency. Specifically, the force is proportional to the rate of change of the power spectral density, evaluated at the resonance frequency. The phenomenon is analogous to the Einstein-Hopf drag on an electric dipole in a fluctuating electromagnetic field.

The effect should also occur for toroidal bubbles, but may exhibit differences when compared to spherical bubbles. For example, because the size of a toroidal bubble (and thus its resonance frequency) continuously changes as

it propagates, the force will not be constant. This observation may offer a dramatic, visual demonstration of the force.

THIS PAGE INTENTIONALLY LEFT BLANK

APPENDIX A. BURKERT SOLENOID VALVE TRIALS

Each table shows tabulated results from a unique combination of nitrogen pressure and nozzle diameter. The data in each table are compiled from a group of nitrogen bursts spaced at 10 second intervals. The following symbols are used to qualitatively rate these pressure-nozzle combinations:

- • one toroidal bubble generated, excellent shape, reaches the top surface intact
- o one toroidal bubble generated, degenerative, does not reach the top surface intact
- •o two toroidal bubbles generated, excellent shape, one toroidal bubble reaches the top surface intact
- oo two toroidal bubbles generated, degenerative, do not reach the top surface intact
- x no toroidal bubble generated

4.0" tube length (±.05")	0.090" inner diameter (±.0005")			
2 *psi* in pressure reservoir	1.75" of tubing between pressure reservoir and solenoid valve			
•	o	•o	oo	x
02	38	00	00	10

4.0" tube length (±.05")	0.130" inner diameter (±.0005")			
2 *psi* in pressure reservoir	1.75" of tubing between pressure reservoir and solenoid valve			
•	o	•o	oo	x
12	11	26	01	00

4.0" tube length (±.05")	0.152" inner diameter (±.0005")			
2 *psi* in pressure reservoir	1.75" of tubing between pressure reservoir and solenoid valve			
•	o	•o	oo	x
21	29	00	00	00

4.0" tube length (±.05")	0.181" inner diameter (±.0005")			
2 *psi* in pressure reservoir	1.75" of tubing between pressure reservoir and solenoid valve			
•	o	•o	oo	x
39	09	00	00	02

4.0" tube length (±.05")	0.090" inner diameter (±.0005")			
4 *psi* in pressure reservoir	1.75" of tubing between pressure reservoir and solenoid valve			
•	○	•○	○○	x
09	29	00	00	12

4.0" tube length (±.05")	0.130" inner diameter (±.0005")			
4 *psi* in pressure reservoir	1.75" of tubing between pressure reservoir and solenoid valve			
•	○	•○	○○	x
10	28	02	00	10

4.0" tube length (±.05")	0.152" inner diameter (±.0005")			
4 *psi* in pressure reservoir	1.75" of tubing between pressure reservoir and solenoid valve			
•	○	•○	○○	x
16	23	01	00	10

4.0" tube length (±.05")	0.181" inner diameter (±.0005")			
4 *psi* in pressure reservoir	1.75" of tubing between pressure reservoir and solenoid valve			
•	o	•o	oo	x
14	28	00	02	06

4.0" tube length (±.05")	0.090" inner diameter (±.0005")			
6 *psi* in pressure reservoir	1.75" of tubing between pressure reservoir and solenoid valve			
•	o	•o	oo	x
12	31	00	00	07

4.0" tube length (±.05")	0.130" inner diameter (±.0005")			
6 *psi* in pressure reservoir	1.75" of tubing between pressure reservoir and solenoid valve			
•	o	•o	oo	x
13	26	00	06	05

4.0" tube length (±.05")	0.152" inner diameter (±.0005")			
6 *psi* in pressure reservoir	1.75" of tubing between pressure reservoir and solenoid valve			
•	○	•○	○○	x
17	26	00	00	07

4.0" tube length (±.05")	0.181" inner diameter (±.0005")			
6 *psi* in pressure reservoir	1.75" of tubing between pressure reservoir and solenoid valve			
•	○	•○	○○	x
27	15	01	00	07

4.0" tube length (±.05")	0.090" inner diameter (±.0005")			
8 *psi* in pressure reservoir	1.75" of tubing between pressure reservoir and solenoid valve			
•	○	•○	○○	x
17	30	00	00	03

4.0" tube length (±.05")	0.130" inner diameter (±.0005")			
8 *psi* in pressure reservoir	1.75" of tubing between pressure reservoir and solenoid valve			
•	o	•o	oo	x
12	28	01	00	09

4.0" tube length (±.05")	0.152" inner diameter (±.0005")			
8 *psi* in pressure reservoir	1.75" of tubing between pressure reservoir and solenoid valve			
•	o	•o	oo	x
16	29	01	00	04

4.0" tube length (±.05")	0.181" inner diameter (±.0005")			
8 *psi* in pressure reservoir	1.75" of tubing between pressure reservoir and solenoid valve			
•	o	•o	oo	x
13	20	00	00	17

4.0" tube length (±.05")	0.090" inner diameter (±.0005")			
10 *psi* in pressure reservoir	1.75" of tubing between pressure reservoir and solenoid valve			
•	○	●○	○○	x
13	32	00	00	05

4.0" tube length (±.05")	0.130" inner diameter (±.0005")			
10 *psi* in pressure reservoir	1.75" of tubing between pressure reservoir and solenoid valve			
•	○	●○	○○	x
07	32	00	02	09

4.0" tube length (±.05")	0.152" inner diameter (±.0005")			
10 *psi* in pressure reservoir	1.75" of tubing between pressure reservoir and solenoid valve			
•	○	●○	○○	x
17	23	00	02	08

4.0" tube length (±.05")	0.181" inner diameter (±.0005")			
10 *psi* in pressure reservoir	1.75" of tubing between pressure reservoir and solenoid valve			
•	o	•o	oo	x
04	17	01	07	21

4.0" tube length (±.05")	0.090" inner diameter (±.0005")			
12 *psi* in pressure reservoir	1.75" of tubing between pressure reservoir and solenoid valve			
•	o	•o	oo	x
18	26	00	00	06

4.0" tube length (±.05")	0.130" inner diameter (±.0005")			
12 *psi* in pressure reservoir	1.75" of tubing between pressure reservoir and solenoid valve			
•	o	•o	oo	x
13	28	00	03	06

4.0" tube length (±.05")	0.152" inner diameter (±.0005")			
12 *psi* in pressure reservoir	1.75" of tubing between pressure reservoir and solenoid valve			
•	○	•○	○○	x
18	22	01	03	06

4.0" tube length (±.05")	0.181" inner diameter (±.0005")			
12 *psi* in pressure reservoir	1.75" of tubing between pressure reservoir and solenoid valve			
•	○	•○	○○	x
03	17	01	14	15

4.0" tube length (±.05")	0.090" inner diameter (±.0005")			
14 *psi* in pressure reservoir	1.75" of tubing between pressure reservoir and solenoid valve			
•	○	•○	○○	x
20	24	00	00	06

4.0" tube length (±.05")	0.130" inner diameter (±.0005")			
14 *psi* in pressure reservoir	1.75" of tubing between pressure reservoir and solenoid valve			
•	o	•o	oo	x
17	26	00	00	07

4.0" tube length (±.05")	0.152" inner diameter (±.0005")			
14 *psi* in pressure reservoir	1.75" of tubing between pressure reservoir and solenoid valve			
•	o	•o	oo	x
11	24	01	03	11

4.0" tube length (±.05")	0.181" inner diameter (±.0005")			
14 *psi* in pressure reservoir	1.75" of tubing between pressure reservoir and solenoid valve			
•	o	•o	oo	x
03	16	01	10	20

APPENDIX B. SKINNER SOLENOID VALVE TRIALS

Each table shows tabulated results from a unique combination of nitrogen pressure and nozzle diameter. The data in each table are compiled from a group of nitrogen bursts spaced at 10 second intervals. The following symbols are used to qualitatively rate these pressure-nozzle combinations:

- ● one toroidal bubble generated, excellent shape, reaches the top surface intact
- o one toroidal bubble generated, degenerative, does not reach the top surface intact
- ●o two toroidal bubbles generated, excellent shape, one toroidal bubble reaches the top surface intact
- oo two toroidal bubbles generated, degenerative, do not reach the top surface intact
- x no toroidal bubble generated

4.0" tube length (±.05")	0.090" inner diameter (±.0005")			
2 *psi* in pressure reservoir	1.75" of tubing between pressure reservoir and solenoid valve			
●	o	●o	oo	x
13	26	00	00	11

4.0" tube length (±.05")	0.130" inner diameter (±.0005")			
2 *psi* in pressure reservoir	1.75" of tubing between pressure reservoir and solenoid valve			
•	o	•o	oo	x
00	00	00	00	50

4.0" tube length (±.05")	0.152" inner diameter (±.0005")			
2 *psi* in pressure reservoir	1.75" of tubing between pressure reservoir and solenoid valve			
•	o	•o	oo	x
25	16	00	00	09

4.0" tube length (±.05")	0.181" inner diameter (±.0005")			
2 *psi* in pressure reservoir	1.75" of tubing between pressure reservoir and solenoid valve			
•	o	•o	oo	x
47	00	00	00	03

4.0" tube length (±.05")	0.090" inner diameter (±.0005")			
4 *psi* in pressure reservoir	1.75" of tubing between pressure reservoir and solenoid valve			
•	o	•o	oo	x
15	24	00	00	11

4.0" tube length (±.05")	0.130" inner diameter (±.0005")			
4 *psi* in pressure reservoir	1.75" of tubing between pressure reservoir and solenoid valve			
•	o	•o	oo	x
30	18	00	00	02

4.0" tube length (±.05")	0.152" inner diameter (±.0005")			
4 *psi* in pressure reservoir	1.75" of tubing between pressure reservoir and solenoid valve			
•	o	•o	oo	x
28	14	00	00	08

4.0" tube length (±.05")	0.181" inner diameter (±.0005")			
4 *psi* in pressure reservoir	1.75" of tubing between pressure reservoir and solenoid valve			
•	o	•o	oo	x
32	14	00	00	04

4.0" tube length (±.05")	0.090" inner diameter (±.0005")			
6 *psi* in pressure reservoir	1.75" of tubing between pressure reservoir and solenoid valve			
•	o	•o	oo	x
21	20	00	00	09

4.0" tube length (±.05")	0.130" inner diameter (±.0005")			
6 *psi* in pressure reservoir	1.75" of tubing between pressure reservoir and solenoid valve			
•	o	•o	oo	x
25	19	00	00	06

4.0" tube length (±.05")	0.152" inner diameter (±.0005")			
6 *psi* in pressure reservoir	1.75" of tubing between pressure reservoir and solenoid valve			
●	○	●○	○○	x
22	23	00	00	05

4.0" tube length (±.05")	0.181" inner diameter (±.0005")			
6 *psi* in pressure reservoir	1.75" of tubing between pressure reservoir and solenoid valve			
●	○	●○	○○	x
39	07	00	00	04

4.0" tube length (±.05")	0.090" inner diameter (±.0005")			
8 *psi* in pressure reservoir	1.75" of tubing between pressure reservoir and solenoid valve			
●	○	●○	○○	x
13	25	00	00	12

4.0" tube length (±.05")	0.130" inner diameter (±.0005")			
8 *psi* in pressure reservoir	1.75" of tubing between pressure reservoir and solenoid valve			
●	○	●○	○○	X
17	21	00	00	12

4.0" tube length (±.05")	0.152" inner diameter (±.0005")			
8 *psi* in pressure reservoir	1.75" of tubing between pressure reservoir and solenoid valve			
●	○	●○	○○	X
21	19	01	00	09

4.0" tube length (±.05")	0.181" inner diameter (±.0005")			
8 *psi* in pressure reservoir	1.75" of tubing between pressure reservoir and solenoid valve			
●	○	●○	○○	X
29	15	00	00	06

4.0" tube length (±.05")	0.090" inner diameter (±.0005")			
10 *psi* in pressure reservoir	1.75" of tubing between pressure reservoir and solenoid valve			
●	○	●○	○○	x
18	21	00	00	11

4.0" tube length (±.05")	0.130" inner diameter (±.0005")			
10 *psi* in pressure reservoir	1.75" of tubing between pressure reservoir and solenoid valve			
●	○	●○	○○	x
20	20	00	00	10

4.0" tube length (±.05")	0.152" inner diameter (±.0005")			
10 *psi* in pressure reservoir	1.75" of tubing between pressure reservoir and solenoid valve			
●	○	●○	○○	x
13	20	00	03	14

4.0" tube length (±.05")	0.181" inner diameter (±.0005")			
10 *psi* in pressure reservoir	1.75" of tubing between pressure reservoir and solenoid valve			
•	o	•o	oo	x
14	21	00	00	15

4.0" tube length (±.05")	0.090" inner diameter (±.0005")			
12 *psi* in pressure reservoir	1.75" of tubing between pressure reservoir and solenoid valve			
•	o	•o	oo	x
21	22	00	00	07

4.0" tube length (±.05")	0.130" inner diameter (±.0005")			
12 *psi* in pressure reservoir	1.75" of tubing between pressure reservoir and solenoid valve			
•	o	•o	oo	x
19	20	00	01	10

4.0" tube length (±.05")	0.152" inner diameter (±.0005")			
12 *psi* in pressure reservoir	1.75" of tubing between pressure reservoir and solenoid valve			
●	○	●○	○○	x
08	23	00	02	17

4.0" tube length (±.05")	0.181" inner diameter (±.0005")			
12 *psi* in pressure reservoir	1.75" of tubing between pressure reservoir and solenoid valve			
●	○	●○	○○	x
03	21	00	01	25

4.0" tube length (±.05")	0.090" inner diameter (±.0005")			
14 *psi* in pressure reservoir	1.75" of tubing between pressure reservoir and solenoid valve			
●	○	●○	○○	x
24	13	00	00	13

4.0" tube length (±.05")	0.130" inner diameter (±.0005")			
14 *psi* in pressure reservoir	1.75" of tubing between pressure reservoir and solenoid valve			
•	o	•o	oo	x
19	18	00	00	13

4.0" tube length (±.05")	0.152" inner diameter (±.0005")			
14 *psi* in pressure reservoir	1.75" of tubing between pressure reservoir and solenoid valve			
•	o	•o	oo	x
05	19	01	03	22

4.0" tube length (±.05")	0.181" inner diameter (±.0005")			
14 *psi* in pressure reservoir	1.75" of tubing between pressure reservoir and solenoid valve			
•	o	•o	oo	x
02	17	00	06	25

LIST OF REFERENCES

Acheson, D. J., *Elementary Fluid Dynamics*, Oxford, 1990, pp. 168-169.

Batchelor, G. K., *An Introduction to Fluid Dynamics*, Cambridge University Press, 1967, pp. 522-526.

Blake, John R.; Keen, Giles S.; Tong, Robert P.; and Wilson, Miles, "Acoustic Cavitation: The Fluid Dynamics of Non-spherical Bubbles," *Philosophical Trans. of the Royal Society of London*, vol. A357, pp. 251-267, 1999.

Chen, Li; Garimella, Suresh V.; Reizes, John A.; and Leonardi, Eddie, "The Development of a Bubble Rising in a Viscous Liquid," *Journal of Fluid Mechanics*, vol. 387, pp. 61-96, 1999 (and references therein).

Faber, T. E., *Fluid Dynamics for Physicists*, Cambridge University Press, 1995, pp. 415-423.

Fitzgerald, Richard, "An Optical Spoon Stirs up Vortices in a Bose-Einstein Condensate," *Physics Today*, pp. 19-21, Aug. 2000.

Lamb, Horace, *Hydrodynamics*, 6th Edition, Cambridge University Press, 1997, ch. 7.

Larraza, A. and Tucholski, E., "Acoustic Einstein-Hopf Drag on a Bubble," *Physics Rev. Lett.* 84, pp. 2378-2380, 2000.

Lundgren, T .S. and Mansour, N. N., "Vortex Ring Bubbles," *Journal of Fluid Mechanics*, vol. 224, pp. 177-196, 1991.

Marten, Ken; Shariff, Karim; Psarakos, Suchi; and White, Don J., "Ring Bubbles of Dolphins," *Scientific American*, pp. 83-87, Aug. 1996.

Metzer, Stephen M.; Carr, James R.; Johnson, Jeffrey R.; Parker, Timothy J.; and Lemmon, Mark T., "Techniques for Identifying Dust Devils in Mars Pathfinder Images," *IEEE Transcripts on Geoscience and Remote Sensing*, vol. 38, pp. 870-876, 2000.

Pedley, T. J., "The Toroidal Bubble," *Journal of Fluid Mechanics*, vol. 32, part 1, pp. 97-112, 1968.

Putterman, Seth J., *Superfluid Hydrodynamics*, North-Holland/American Elsevier, 1974, pp. 7-9, 32-34, 72-78, 163-177, 181-194, 251-262, 309-330; ch.2, app. V.

Rief, F., "Quantized Vortex Rings in Superfluid Helium," *Scientific American*, pp. 116-122, Dec. 1964.

Semper, Robert J., "Toroidal Bubbles," *Nature*, vol. 356, p. 390, 1992.

Shankar, P. N. and Kumar, Manoj, "Toroidal Vortex Rings," *Current Science*, vol. 66, pp. 151-153, 1995.

Sussman, Mark and Smereka, Peter, "Axisymmetric Free Boundary Problems," *Journal of Fluid Mechanics*, vol. 341, pp. 269-294, 1997.

Turner, J. S., "Buoyant Vortex Rings," *Proceedings of the Royal Society*, vol. A239, pp. 61-75, 1957.

Walters, J. K. and Davidson, J. F., "The Initial Motion of a Gas Bubble Formed in an Inviscid Liquid – Part 2: The Three-dimensional Bubble and the Toroidal Bubble," *Journal of Fluid Mechanics*, vol. 17, pp. 321-336, 1963.

INITIAL DISTRIBUTION LIST

1. Defense Technical Information Center 2
   8725 John J. Kingman Road, Suite 0944
   Fort Belvoir, Virginia 22060-6218

2. Dudley Knox Library 2
   Naval Postgraduate School
   411 Dyer Road
   Monterey, California 93943-5101

3. Professor Bruce C. Denardo, Code PH/Db 3
   Department of Physics
   Naval Postgraduate School
   Monterey, California 93943-5002

4. Professor Andrés Larraza, Code PH/La 1
   Department of Physics
   Naval Postgraduate School
   Monterey, California 93943-5002

5. Undersea Warfare Programs Office, Code 35 1
   Naval Postgraduate School
   833 Dyer Road, Room 304
   Monterey, California 93943-5124

6. Scott Billets 1
   24809 Santa Rita Street
   Carmel, California 93923

7. Galen Blackwell 1
   857 Grove Acres
   Pacific Grove, California 93950

8. Allen L. Hobbs 3
   121 Edgewater Circle
   San Benito, Texas 78586

9. Larry Hobbs 1
   15255 Kamary Lane
   San Antonio, Texas 78247